# Structure and host–actinomycete interactions in developing root nodules of *Comptonia peregrina*

WILLIAM NEWCOMB[1] AND R. L. PETERSON

*Department of Botany and Genetics, University of Guelph, Guelph, Ont., Canada N1G 2W1*

AND

DALE CALLAHAM AND JOHN G. TORREY

*Cabot Foundation, Harvard University, Petersham, MA, U.S.A. 01366*

Received June 29, 1977

NEWCOMB, W., R. L. PETERSON, D. CALLAHAM, and J. G. TORREY. 1978. Structure and host–actinomycete interactions in developing root nodules of *Comptonia peregrina*. Can. J. Bot. **56**: 502–531.

Correlated fluorescence, bright-field, transmission electron, and scanning electron microscopic studies were made on developing root nodules of *Comptonia peregrina* (L.) Coult. (Myricaceae) produced by a soil actinomycete which invades the root and establishes a symbiosis leading to fixation of atmospheric dinitrogen. After entering the host via a root hair infection, the hyphae of the endophyte perforate root cortical cells by local degradation of host cell walls and penetration of the host cytoplasm. The intracellular hyphae are always surrounded by host plasma membrane and a thick polysaccharide material termed the capsule. (For convenience, term intracellular refers to the endophyte being inside a *Comptonia* cell as distinguished from being intercellular, i.e., between host cells, even though the former is actually extracellular as the endophyte is separated from the host cytoplasm by the host plasmalemma.) Numerous profiles of vesiculate rough endoplasmic reticulum (RER) occur near the growing hyphae. Although the capsule shows a positive Thiery reaction indicating its polysaccharide nature, the fibrillar contents of the RER do not, leaving uncertain whether the capsule results from polymers derived from the RER. Amyloplasts of the cortical cells lose their starch deposits during hyphal proliferation. The hyphae branch extensively in specific layers of the cortex, penetrating much of the host cytoplasm. At this stage, hyphal ends become swollen and form septate club-shaped vesicles within the periphery of the host cells. Lipid-like inclusions and Thiery-positive particles, possibly glycogen, are observed in the hyphae at this time. Associated with hyphal development is an increase in average host cell volume, although nuclear volume appears to remain constant. Concomitant with vesicle maturation, the mitochondrial population increases sharply, suggesting a possible relationship to vesicle function. The intimate interactions between host and endophyte during development of the symbiotic relationship are emphasized throughout.

---

NEWCOMB, W., R. L. PETERSON, D. CALLAHAM et J. G. TORREY. 1978. Structure and host–actinomycete interactions in developing root nodules of *Comptonia peregrina*. Can. J. Bot. **56**: 502–531.

Les auteurs ont réuni les techniques de la microscopie photonique, en fluorescence et sur fond clair, ainsi que de la microscopie électronique par transmission et à balayage, pour étudier le développement des nodules racinaires chez le *Comptonia peregrina* (L.) Coult. (Myricaceae), à la suite d'une invasion des racines par une actinomycète du sol, lequel entraîne la formation d'une symbiose qui conduit à la fixation de l'azote atmosphérique. Après être entrés dans l'hôte en infectant un poil absorbant, les hyphes de l'endophyte perforent les cellules corticales de la racine en dégradant localement les parois cellulaires de l'hôte et pénètrent subséquemment dans son cytoplasme. Les hyphes intracellulaires sont toujours entourés par le plasmalemme de l'hôte ainsi que par un matériel polysaccharidique épais appelé la capsule. On observe, au voisinage de l'hyphe en croissance, de nombreux profils de reticulum endoplasmique rugueux (RER) vésiculeux. Bien que la capsule soit positive au réactif de Thiery, dénotant sa nature polysaccharidique, les contenus fibrillaires du RER ne le sont pas ce qui laisse planer un doute sur la possibilité que les polymères de la capsule proviennent du RER. Au cours de la prolifération des hyphes, les amyloplastes de cellules corticales perdent leurs réserves d'amidon. Les hyphes se ramifient extensivement dans certaines couches du cortex et pénètrent une bonne partie du cytoplasme de l'hôte. A ce stade, les extrémités des hyphes se gonflent et forment des vésicules allongées à la périphérie du cytoplasme des cellules hôtes. Des inclusions d'apparence lipidique et des particules positives au réactif de Thiery, possiblement du glycogène, se retrouvent dans les hyphes à ce stade. Au cours du développement de l'hyphe on note une augmentation du volume moyen de la cellule de l'hôte bien que le volume nucléaire semble demeurer constant. Simultané-

[1]Present address: Department of Biology, Queen's University, Kingston, Ont., Canada K7L 3N6.

ment à la maturation des vésicules, la population de mitochondries augmente fortement ce qui suggère une relation possible avec le fonctionnement des vésicules. Les auteurs insistent sur les interactions étroites qui existent entre l'hôte et son endophyte tout au long de l'établissement de la relation symbiotique.

[Traduit par le journal]



## Introduction

*Comptonia peregrina* (L.) Coult. (*Myrica asplenifolia*), commonly called sweet fern, is a nonleguminous angiosperm bearing nitrogen-fixing root nodules which contain an actinomycete-like organism (Becking 1975, 1977; Bond 1974, 1976*a*). The resulting symbiosis,which leads to the fixation of molecular nitrogen (Ziegler 1960; Ziegler and Hüser 1963; Stewart *et al.* 1967; Fessenden *et al.* 1973), allows *Comptonia* to carry out a pioneering role in the revegetation of denuded land. It is commonly planted along highways in Massachusetts for this purpose.

In view of the wide distribution of the 157 species of angiosperms having root nodule symbioses with actinomycete-like organisms (Bond 1976*a*) it is surprising that most of the research has involved the genus *Alnus*. Consequently there have been many ultrastructural studies of *Alnus* nodules (Becking *et al.* 1964; Gardner 1965; Lalonde and Knowles 1975*a*, 1975*b*; Lalonde and Devoe 1976; Van Dijk and Merkus 1976) and fewer studies of the remaining genera. The nodules of *Hippophaë rhamnoides* have been studied (Gatner and Gardner 1970; Gardner and Gatner 1973). *Myrica cerifera* nodules were first described by Silver (1964) and studied again by Gardner (1976), who also showed some ultrastructural details in the nodules of *M. gale*, *Ceanothus velutinus*, and *Casuarina cunninghamiana*. Chandler and Dart (1971) briefly reported on the endophyte of *Casuarina*, while the nodules of *Colletia paradoxa* and *Purshia tridentata* have been carefully examined by Bond (1976*a*, 1976*b*).

As part of a research program on nodule development in legumes (Newcomb 1976; Syōno *et al.* 1976; Newcomb *et al.* 1977) and nonleguminous species (Torrey 1976; Bowes *et al.* 1977; Callaham and Torrey 1977), a project to study the fine structure of *Comptonia* root nodules was initiated. This paper describes the anatomy and fine structure of developing *Comptonia* root nodules with emphasis on the development of the endophyte and the infected host cells in relation to the whole nodule. Observations based on bright-field and fluorescence light microscopy are correlated with scanning (SEM) and transmission electron microscopy (TEM) in this investigation.

## Materials and Methods

*Plant Material*

Seeds of *Comptonia peregrina* were collected prior to fruit abscission, scarified, soaked for 24 h in 500 ppm gibberellic acid ($GA_3$) (Del Tredici and Torrey 1976), and planted in washed sand. Young seedlings were transplanted to aeroponic culture tanks (Zobel *et al.* 1976) and inoculated with suspensions prepared from old root nodules taken from *Comptonia* plants also grown in aeroponic culture; thus, this inoculum was much cleaner than if taken from the nodules of soil-grown plants. The seedlings were placed with roots suspended in a mist of one-eighth-strength Hoagland's solution (Hoagland and Arnon 1950) lacking nitrogen, and were grown in the greenhouse at Harvard Forest with day and night minimum temperatures of 21°C and 16°C respectively.

*Tissue Preparation for Light and Transmission Electron Microscopy*

Young nodules, 2–3 weeks after inoculation, were fixed in 2.5% glutaraldehyde in 0.025 *M* cacodylate buffer at room temperature for 2–4 h. After rinsing several times in buffer, the tissue was postfixed in 1% osmium tetroxide on ice for 2–4 h, washed several times with buffer, slowly dehydrated in 10% increments of acetone, and (flat) embedded in Araldite (Newcomb 1976). Initially, many other fixation schedules were tried without success on tissue obtained from older nodules (which were also difficult to section). Younger nodules which generally contain fewer deposits of phenolic compounds than older nodules, can be fixed and sectioned relatively easily. Phenolics and tannins may hinder good fixation and thin sectioning as suggested by Gardner (1976) on the basis of her studies with root nodules of nonleguminous species.

*Staining and Histochemistry*

Sections for light microscopy were cut at 0.5–1.0 microns (μm) and stained with 0.05% toluidine blue O in 1% sodium tetraborate (borax) over an alcohol lamp. Sections for transmission electron microscopy (TEM) were cut with glass knives, stained for 30 min with a saturated solution of uranyl acetate in 50% ethanol followed by 5–10 min in 0.02% lead citrate (Venable and Coggleshall 1965), and examined with a Philips EM 200 microscope.

Histochemical techniques for the demonstration of carbohydrates were also carried out. For bright-field light microscopy, sections were stained by the periodic acid–Schiff's technique (Feder and O'Brien 1968); however, the wall material surrounding the endophyte was too thin to permit enough reaction for photomicrography. To utilize the additional sensitivity of the epifluorescence microscope, 0.5 μm sections were mounted on glass slides, placed in sodium methoxide (Erlandson *et al.* 1973) for 45 min to remove the Araldite, rinsed in 1% periodic acid for 10 min, stained with the fluorescent Schiff reagent (Culling 1974), examined with a Leitz epifluorescence microscope using a broad band filter system (BG12 exciting filter and a K515 suppression filter), and photographed using Kodak Tri-X film. Cell walls, starch grains, and other polysaccharides fluoresced a bright yellow–gold color. For TEM, gold-color sections were placed on stainless steel grids and stained for the Thiery reaction using the periodic acid – thiocarbohydrazide (TCH) – silver

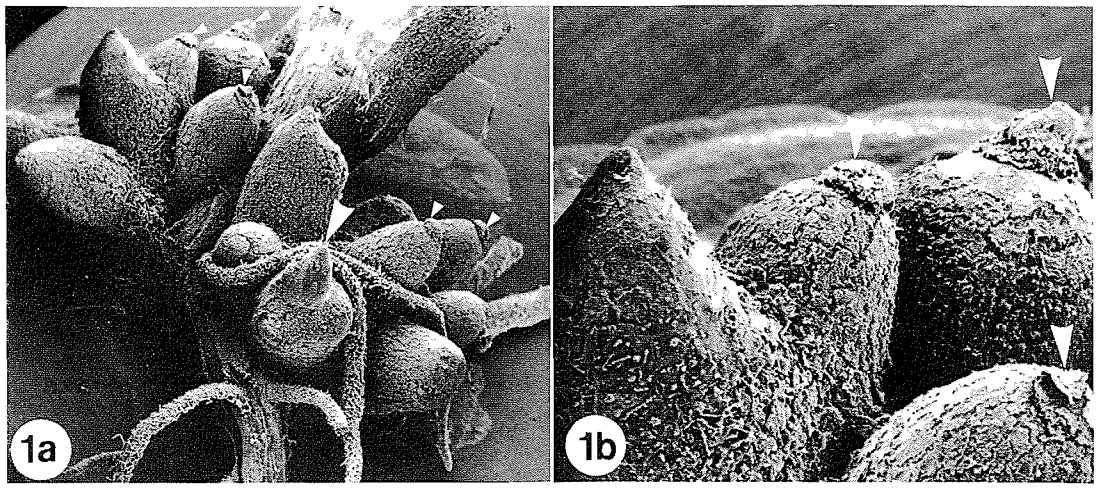


ABBREVIATIONS USED ON FIGURES: A, amyloplast; B, branch of hypha; BEH, broken endophyte hypha; C, capsule; Co, cortex; Cp, cell plate; CW, cell wall; DS, dense substance; EVe, early vesicle; EH, encapsulated hypha; F, fibril; G, granule; H, hypha; HC, heterochromatin; IS, intercellular space; L, lipid; M, mitochondrion; MVB, multivesicular body; N, nucleus; Nc, nucloid; NH, newly infected cells; NM, nodule lobe meristem; Nu, nucleolus; P, proplastid; Pa, papilla; Pd, plasmodesma; Ph, phenol; Pr, perforation; RER, rough endoplasmic reticulum; RH, root hair; S, starch; Sb, striated body; Sp, septum; St, stele; T, tear, UC, uninfected cells; V, vacuole; Ve, vesicle.

FIG. 1. (*a*). Scanning electron micrograph (SEM) of a multilobed *Comptonia* nodule and the lateral root to which the nodule lobes are attached. A cap-like structure, the papilla (small arrows) is evident at the tips of some nodule lobes. A young nodule root (large arrow) lacking a papilla is shown. × 80. (*b*). Higher magnification of four nodule lobes, illustrated in Fig. 1*a*, three of which have prominent papillae (arrows) at their tips. Root hairs are evident at lower left. × 230.

proteinate method (Freundlich and Robards 1974). Three controls were used: first, oxidation in periodic acid not followed by TCH but stained with silver proteinate; second, no treatment with either periodic acid or TCH prior to staining with silver proteinate; and third, no oxidation by periodic acid but treated with TCH and silver proteinate. Fine electron-dense silver particles occurred over carbohydrates in the treatment but not in any of the controls.

*Tissue Preparation for Scanning Electron Microscopy*

Whole nodules and nodule slices were fixed in 2% glutaraldehyde and 0.5% osmium tetroxide in distilled water at room temperature for 1 to 2 h, washed 5 times in distilled water at room temperature for 1 h, placed in 1% TCH for 15 min, rewashed, postfixed in 0.5% osmium tetroxide in distilled water at room temperature for 1 h, rewashed, dehydrated over 3 h in acetone, and dried by the critical point method (Kelly *et al.* 1973). The preparations were mounted on stubs, coated with gold and palladium with a Techon Hummer II sputterer and examined with an ETEC scanning electron microscope. It was necessary to retrim the specimen so that cleanly cut cells free of debris were present. Examination of the nodule tissue fixed as slices proved to be difficult because the preserved host cytoplasm obscured the endophyte. Nodules which were fixed whole were sectioned after critical point drying, revealing a white interior, indicating that the osmium did not penetrate to the inside of the organ. These preparations were coated and subsequent examinations revealed many infected cells in which the endophyte was not obscured by the host cytoplasm although phenolic deposits and starch grains were still present.

## Results

*External Structure*

The root nodules of *Comptonia* are structurally complex. The nodules, which may attain a diameter of several centimetres, are comprised of numerous swollen, radially symmetrical, pointed lobes from whose tips negatively geotropic roots grow (Figs. 1*a* and *b*). Such roots are referred to as nodule roots (Bond 1952, 1974) and remain uninfected except at their bases (Torrey 1976). Initially the nodules have only a few lobes, but endophyte stimulated proliferation of cortical, pericycle, and endodermis cells in the adjacent root tissue results in the formation of more nodule lobes (Bowes *et al.* 1977; Callaham and Torrey 1977).

*Tissue Organization*

While the arrangement of tissues within each nodule lobe shows many similarities to those occurring in normal roots, there are some obvious and important differences. Each nodule lobe contains a meristematic area (the nodule lobe meristem) located near the tip or distal end (Fig. 2). By continued mitotic activity this meristem gives rise to the other tissues: the epidermis, the nodule cortex, and the endodermis surrounding the centrally located vascular cylinder. Only the middle cortical cells of the nodule lobe become infected by the actinomycete (Fig. 2); the cortical cells adjacent to the endodermis and epidermis remain free of the endophyte. Likewise, the endophyte has never been observed in the vacular tissues, the nodule

lobe meristem, or the epidermis (other than in the root hair through which the endophyte enters the root).

The invasion by the endophyte into the root hair, early formation of the prenodule and subsequent spread of the endophyte into cortical tissues of the nodule lobes was described by Callaham and Torrey (1977). By following a series of infected cortical cells basipetally, the developmental sequence of host cell and endophyte differentiation may be observed (Fig. 2). Near the nodule lobe meristem the infected cells are relatively small and the endophyte is hyphal in morphology (Fig. 3). In infected cells progressively more basipetal, the amount of endophyte hyphae increases so that much of the central cytoplasm is invaded by the actinomycete (Figs. 2, 4, 5, 6, 7, 11, 12, 13, 21, and 23). At the periphery of the host cell the hyphal tips become swollen (Figs. 7, 8, 13–16, and 38*a*) and eventually form elongate, club-shaped septate structures termed vesicles (Figs. 9, 10, 17, 40, and 41*b*). The host cells containing the vesicle stage of the endophyte are much larger than the newly infected cortical cells and adjacent uninfected cortical cells (Fig. 2). Many of the uninfected cortical cells contain amyloplasts with large starch granules and large vacuoles with phenolic deposits (Figs. 2, 3, 7, 8, 9, 24, 25, and 41*b*).

The nodule lobe is covered by a tissue comprised of phenol-containing cells in the epidermis and outer layers of the cortex (Fig. 2). At the tips of the nodule lobes this tissue forms a cap-like structure, referred to as a papilla (Bowes *et al.* 1977), which is several cell layers thick because of the activity of the lobe meristem. In *Alnus* this outer covering has been termed a superficial cork layer or periderm (Hawker and Fraymouth 1951; Gardner 1965; Bond 1974; Dalton and Naylor 1975) and in *Myrica gale*, the cork exoderm (Fletcher and Gardner 1974). In young nodule lobes of *Comptonia*, epidermal and cortical tissues remain intact; later a corky layer forms (Callaham and Torrey 1977).

*Development and Differentiation of Infected Cells*

The ontogeny of the infected cells involves mitoses in the nodule meristem, invasion of host cells by the actinomycete-like organism, encapsulation of the endophyte, and growth and differentiation of both the host and endophyte cells.

*Nodule Meristem*

Continued mitotic activity within the nodule lobe meristem is essential for nodule growth since most of the nodule cells are derived from this meristem. Infected nodule cortical cells do not undergo mitosis. The nodule lobe meristem is never invaded by the endophyte but whether this is because mitotic activity of the nodule meristem occurs at a faster rate than growth of the endophyte or because of the existence of subtle physiological barriers to infection is unknown. Typically, nodule lobe meristem cells contain a large nucleus with a single nucleolus, amyloplasts often possessing multiple starch granules, numerous mitochondria with many cristae, small amounts of endoplasmic reticulum, many free ribosomes, a few polysomes, and many small vacuoles (Figs. 2, 3, 26*a*, and 26*b*). Plasmodesmata are common and may be unbranched or branched joining with a median sinus of Mittelknoten (Juniper 1976) located in the middle lamella (Figs. 26*a* and 26*c*). Generally, mitotically active nodule meristem cells are free of or contain only small amounts of phenols (Fig. 26*a*). However, cells with large phenolic deposits, usually located in vacuoles, do occur in and near the nodule meristem (Figs. 2, 3, 24, and 25); occasionally these cells are observed undergoing mitosis (Fig. 25). These cells may remain uninfected because of the presence of these phenolic substances; newly infected cells rarely contain large phenolic deposits (Figs. 3–6 and 27*a*).

*Invasion of the Host Cells*

One of the remarkable aspects of the *Comptonia*–actinomycete symbiosis is the growth of the endophyte through the host cell wall. Structural details of the initial root hair deformation and invasion of the host by the soil-borne organism are to be reported elsewhere. Once inside the epidermal cell, the endophyte grows invasively into cortical tissues, causing cell hypertrophy and cell division in advance of it (Callaham and Torrey 1977). Fluorescence and light microscopic observations (Figs. 3–6, 8, 9, and 11–16) clearly demonstrate the passage of numerous endophyte hyphae through the host cell wall, parallel to the host wall, or in the wall itself. When the hyphae are oriented more or less perpendicular to the host cell wall, they usually pass through the wall without grossly disrupting the shape of the wall (Figs. 4–6, 11–13, 15, and 16), i.e., the host wall is not distorted as would be expected if the penetration of the hyphae were achieved merely by physical force or pressure. When the hyphae are oriented parallel to the host cell wall, there may be some distortion in the wall (Figs. 5 and 6).

In newly infected cells the nucleus and most of the cytoplasm are located in the central region of the host cell (Figs. 3–6, 11, and 12). The hyphae grow through the host cell wall into the central region of cytoplasm (Figs. 5–7, 11, and 12); al-

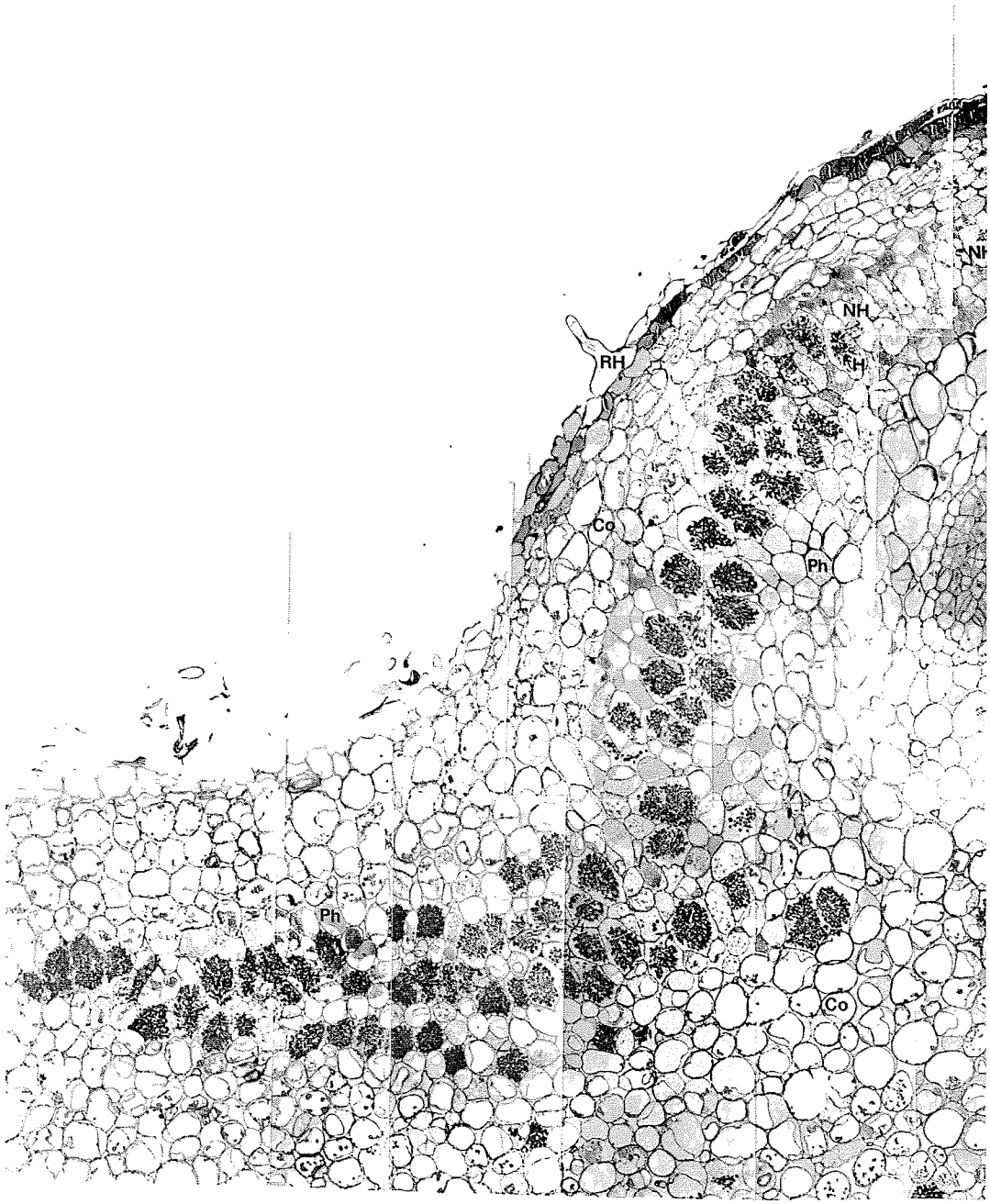


FIG. 2. Light micrograph montage showing two lobes of a young *Comptonia* root nodule. Both the younger, small, medianly sectioned lobe on the right and the older, large, tangentially sectioned lobe on the left illustrate the acropetal pattern of development and differentiation: an uninfected nodule lobe meristem (NM), a region of large uninfected cells derived from the meristem (UC), newly infected cells (NH) containing only a few hyphal strands of endophyte, cells containing more strands of hyphae (H), and cells containing the vesicle (Ve) stage of the endophyte. Note that the infected cortical cells are

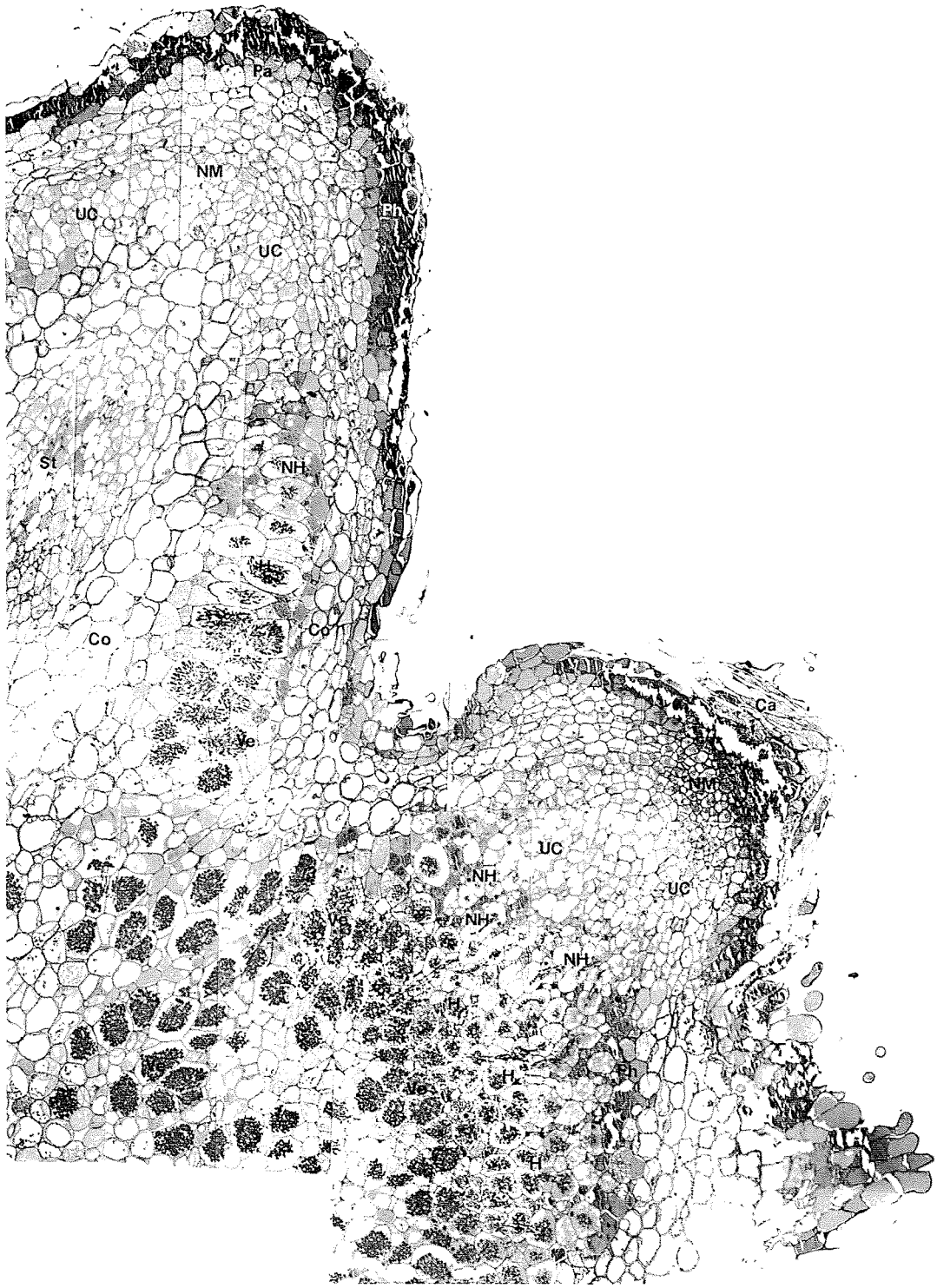


located between two layers of uninfected cortical (Co) cells. The incompletely differentiated stele (St), is seen in the centre of the larger lobe, which in tangential section does not show its connection to the vascular tissue of the root to which it is attached. The infected cells are nearly continuous in their distribution from the base into each nodule lobe. The outer epidermal cells include a root hair (RH) and large phenolic (Ph) deposits. Epidermal cells and derivatives of the meristem form the cap-like structure, the papilla (Pa) at the tip of the nodule lobe. × 165.

though the hyphae often grow near the nucleus, the endophyte was never observed within the host nucleus. In tissue stained with the fluorescent PAS reagent, there is an obvious PAS-positive layer, continuous with the host cell wall, surrounding the endophyte (Figs. 11–17). This layer is called the capsule. As the number of hyphae increases in the central region of cytoplasm, the PAS-positive capsule surrounding the endophyte fuses into one continuous structure (Figs. 11 and 12), which appears flattened in the SEM (Figs. 21 and 22).

TEM observations confirm that hyphae oriented more or less perpendicular to the host cell wall pass through a hole or opening in the host wall, causing a minimum amount of distortion to the host wall itself (Figs. 27*a*, 28, and 29). The endophyte hyphae is bounded by its own plasmalemma and cell wall and is separated from the host cytoplasm by the host-produced capsule and the host plasma membrane (Figs. 33, 35, and 37). The capsule, which completely surrounds the actinomycetous endophyte, is continuous with the host cell wall and is similar to it in density and fibrillar substructure (Figs. 27*b*, 28, 29, and 31*a*). The hyphae oriented parallel to the host cell wall usually grow in the region of the middle lamella between adjacent cell walls (Figs. 28 and 30). Such hyphae may occur in pairs within these walls (Fig. 28); they may also branch within the host cell wall, giving rise to encapsulated hyphae which penetrate another host cell (Fig. 30).

The manner by which the endophyte penetrates the host cell wall is not known. The host cell wall is usually not thinner near the site of hyphal penetration although occasional thin spots are observed at these sites (Fig. 31*a*; Fig. 12 in Callaham and Torrey 1977). Some of the thin spots occur in association with unknown bodies which are bounded by a membrane and contain an electron-dense substance (Figs. 31*a* and 31*b*). In addition, a fibrillar material occasionally is observed at the site of wall degradation (Fig. 31*c*).

SEM studies clearly demonstrate the occurrence of perforations in the host cell wall (Figs. 18–20). These perforations which are of the proper dimensions to accommodate the endophyte hyphae, are numerous and often associated with a cylindrical tube of wall protruding into the cell from the host cell wall (Figs. 18–20). While these tubes probably represent broken hyphal capsules resulting from specimen preparation, the surface of the end is unusually regular for a broken surface (Fig. 20). Growing hyphal tips appear to be tapered (Figs. 21–23). Protrusions of wall material are frequently observed on the wall surfaces of newly infected cells (Figs. 18–20), which may represent endophyte just completing penetration of the host cell wall.

*Encapsulation of the Endophyte*

The intracellular endophyte is always surrounded by the capsule (Figs. 27*a*–41*a*), which is cell wall material similar to that of the host cell wall (Figs. 27*b*–30) and probably produced by host cell organelles. After invasion by the endophyte, the host cell nucleus and nucleolus are similar in size and structure to those observed in uninfected derivatives of the nodule meristem (Figs. 3–9). The host cell has a few amyloplasts with small starch granules, a few proplastids, many mitochondria and free ribosomes, a few polyribosomes, abundant profiles of vesicular rough endoplasmic reticulum (RER), a few Golgi bodies, and numerous small vacuoles (Figs. 3–6, 27*a*, 27*b*, and 32–35). The RER usually contains a fibrillar material (Figs. 27*b*, 29, and 32–35) which often is near or appearing to fuse with the capsule (Figs. 29, 32, and 34). Similarly, multivesicular bodies and smooth vesicles are often located near the capsule (Fig. 29). In sections upon which the Thiery reaction for polysaccharide was performed (Figs. 42–45), the capsule, endophyte and host-cell walls, endophyte septa, starch granules of the amyloplasts, and small electron-dense granules in the endophyte all reacted positively. The vesicular RER did not contain positive reacting substances.

*Hyphal Fine Structure*

The fine structure of the hyphal stage of the actinomycete reveals three distinct regions: a boundary layer of plasma membrane and cell wall; a large

FIG. 3. Light micrograph of newly infected cells with hyphae (H) and uninfected cells near the nodule meristem. Note the low numbers of mitochondria and proplastids (small arrows) in these cells (cf. Figs. 5, 6, and 7) and hypha passing through cell (large arrow). Also shown are cells with phenolic (Ph) deposits. × 1400. FIG. 4. Light micrograph of infected cells with hyphae passing through cell walls (large arrows) and numerous hyphae in the central area of cytoplasm. Note the large number of host organelles (small arrows), mainly mitochondria, which occur near the endophyte, and the increase in host cell size (cf. Fig. 3). × 1330. FIG. 5. Light micrograph of cells illustrating the hyphal (H) stage of the endophyte. When the endophyte passes through cell walls (large single arrows), it causes little distortion to the host wall; however, hyphae can grow between walls in the middle lamella (double large arrow) and distort wall contours. Amyloplasts (single small arrows) are present in uninfected cells. × 1300. FIG. 6. Light micrograph showing four hyphal strands passing through a small area of cell wall (single arrows) without distorting the shape of the host wall. Also shown is a hypha (double arrow) growing in the middle lamella between adjacent cell walls which have become distorted. × 1300.

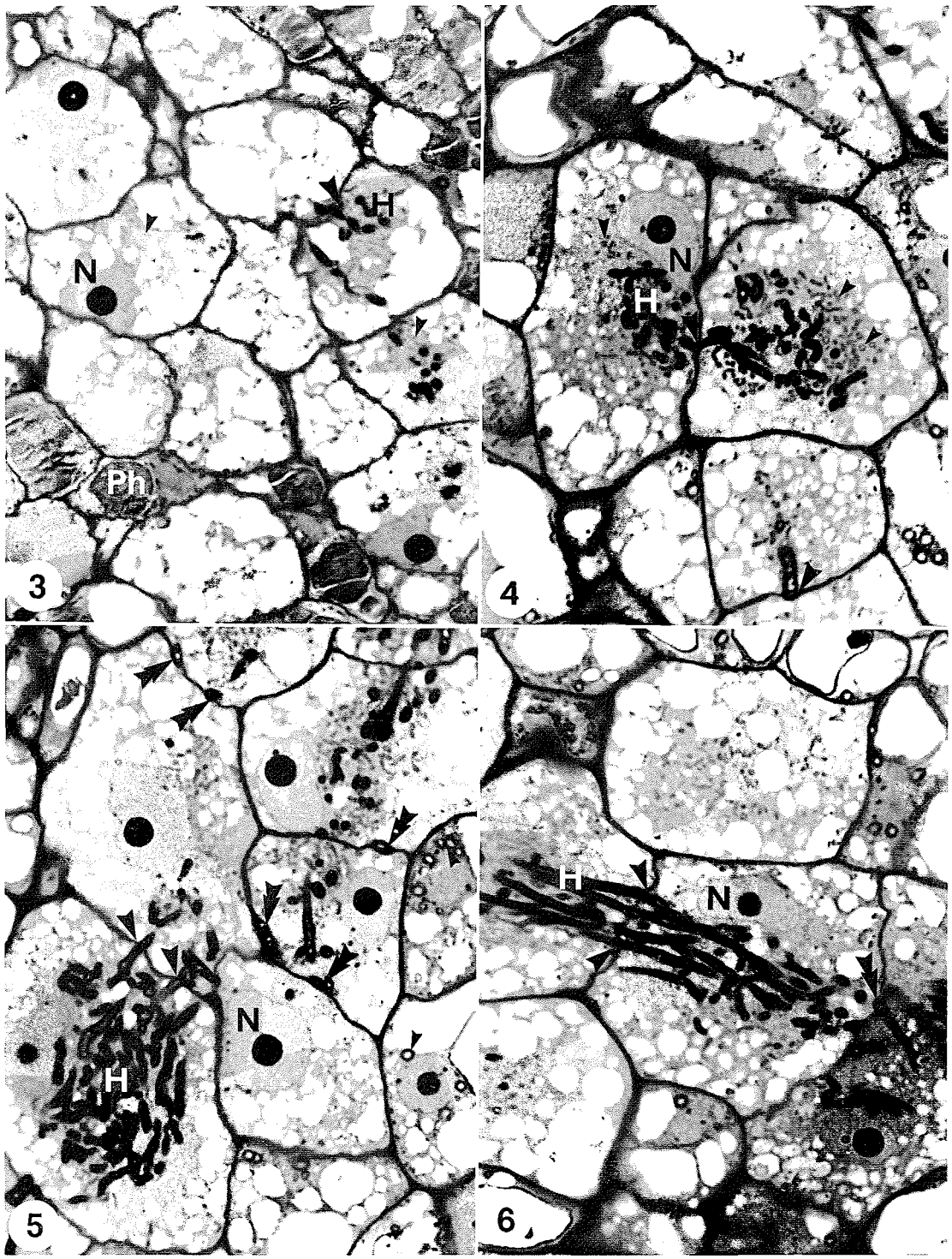

electron-dense area located at the cell periphery containing numerous ribosomes and electron-dense, rosette-shaped granules (probably glycogen); and smaller, centrally located, less dense nucloid regions containing numerous fibrils, presumably DNA, and many vesicles, some of which contain lipid-like substances (Figs. 33, 35–37). The cell wall appears to consist of an inner, less dense layer and an outer, thicker, more dense layer (Figs. 33, 35, and 37). The hyphae contain cross walls or septa which are thicker in the middle than at the ends at the junction with the cell wall (Fig. 37). The septa also contain two different densities of wall material.

*Growth and Differentiation of the Endophyte*

Morphogenesis and growth of the endophyte are responsible for the full ramification of the hyphal stage within the host cytoplasm and the subsequent formation of vesicles, the club-shaped swellings which develop at the ends of the hyphae at the cell periphery. The hyphae frequently branch (Figs. 15, 16, and 30) and bear numerous spherical protuberances along their length (Figs. 21 and 22). Only occasionally are these protuberances located terminally. Since vesicles are only formed at the ends of the hyphae, the laterally occurring protuberances probably are the sites of hyphal branching. Eventually most of the host cytoplasm is occupied by the endophyte hyphae (Figs. 7, 8, and 23).

When the endophyte has penetrated most of the host cytoplasm of infected cortical cells, the hyphae form terminal club-shaped vesicles. The ends of the hyphae increase in diameter and become swollen (Figs. 7, 8, 13–16, 38*a*, and 38*b*). At this stage, the hyphae contain numerous PAS- and Thiery-positive areas (Figs. 13, 14, 16, and 42–45) and areas which are unstained with toluidine blue O (Figs. 7 and 8); in the TEM, numerous small electron-opaque areas occur in the hyphae (Figs. 38*a*, 38*b*, and 39). A few septa occur mainly in the hyphal regions in the central portion of the host cell (Figs. 13, 16, and 38*a*). However, unlike the endophyte occurring in *Hippophaë* nodules (Gardner and Gatner 1973; Gardner 1976), the presumptive vesicle is not separated from the hyphae by a septum. Septa soon begin to form within the developing vesicle which increases in diameter and length (Figs. 14, 41, 42*a*, and 42*b*). The septa which grow toward the center of the hyphae, are often crooked or incomplete as a result of freely growing cell walls. Most of the PAS- and Thiery-positive material and electron-opaque areas are absent when the vesicles are septate (Figs. 14, 15, 17, 44*a*, 44*c*, and 45). The cytoplasm of the vesicles is very electron dense and appears to be devoid of mesosomes (Fig. 46), a characteristic feature of the actinomycetes found in other nonleguminous root nodules. Striated structures similar to the striated bodies observed in *Alnus* and *Hippophaë* (Gardner 1976; Becking 1977) are present in the vesicles (Fig. 46). Small, less dense nucloid regions are present in most of the compartments of the vesicles. The centrally located regions of hyphae contain many areas which appear empty (Fig. 41*a*).

*Changes in Infected Host Cells*

The organelles of the host cell undergo numerous changes during the morphogenesis of the endophyte. The nucleus, which still contains a single prominent nucleolus, becomes lobed, perhaps due in part to the penetration of the surrounding cytoplasm by the endophyte. Many of the previously small vacuoles fuse, forming larger vacuoles located at the periphery of the cell (Figs. 8, 9, 14–17, 38*a*, 40, and 41*a*). Some of these vacuoles contain phenolic compounds (Figs. 40 and 41*a*). A few small vacuoles may still be present in the central portion of the cell (Fig. 41*a*). The mitochondria undergo a tremendous increase in number at about the time that the vesicles become septate (Figs. 40 and 41*a*). Frequently, the mitochondria occur in pairs or in groups of three or four, possibly because of recent divisions (Fig. 41*b*). Often the mitochondria are adjacent to the capsule (Figs. 41*a* and 41*b*), although this may be a function of the extensive ramification of the endophyte which leaves no area of host cytoplasm far removed from it. Very few

FIG. 7. Light micrograph montage showing the transition of the hyphal (H) form to the vesicle (Ve) form of the endophyte. The hyphal stage has penetrated most of the central cytoplasm in the cells at the upper portion of the figure. Swollen hyphal tips (single arrows) denote the beginning of the transition and subsequent growth results in the formation of club-shaped vesicles. The endophyte remains hyphal in the centre of the cell and becomes less dense (i.e., stains less intensely) than earlier stages of the hyphae or the vesicles. Numerous small nonstaining areas (double arrows) form in endophyte during vesicle formation. Uninfected cells contain amyloplasts (A) and phenolics (Ph) and are smaller than infected cells. × 1600. FIG. 8. Light micrograph of cells containing immature vesicles (single small arrows) and mature vesicles (double small arrows). Note endophyte passing through cell wall (single large arrows). × 1230. FIG. 9. Light micrograph of two adjacent cells containing endophyte with vesicles (small arrows) and two adjacent hyphae (single large arrows) passing through the host cell wall with a minimum of distortion. Two vesicles (double large arrows) are clearly continuous with the central hyphae. × 880. FIG. 10. Light micrograph of infected cells containing vesicle (Ve) stage of endophyte. Vesicles are continuous (large arrows) with hyphal (H) strands. The central hyphae cut in transection appear empty. × 780.

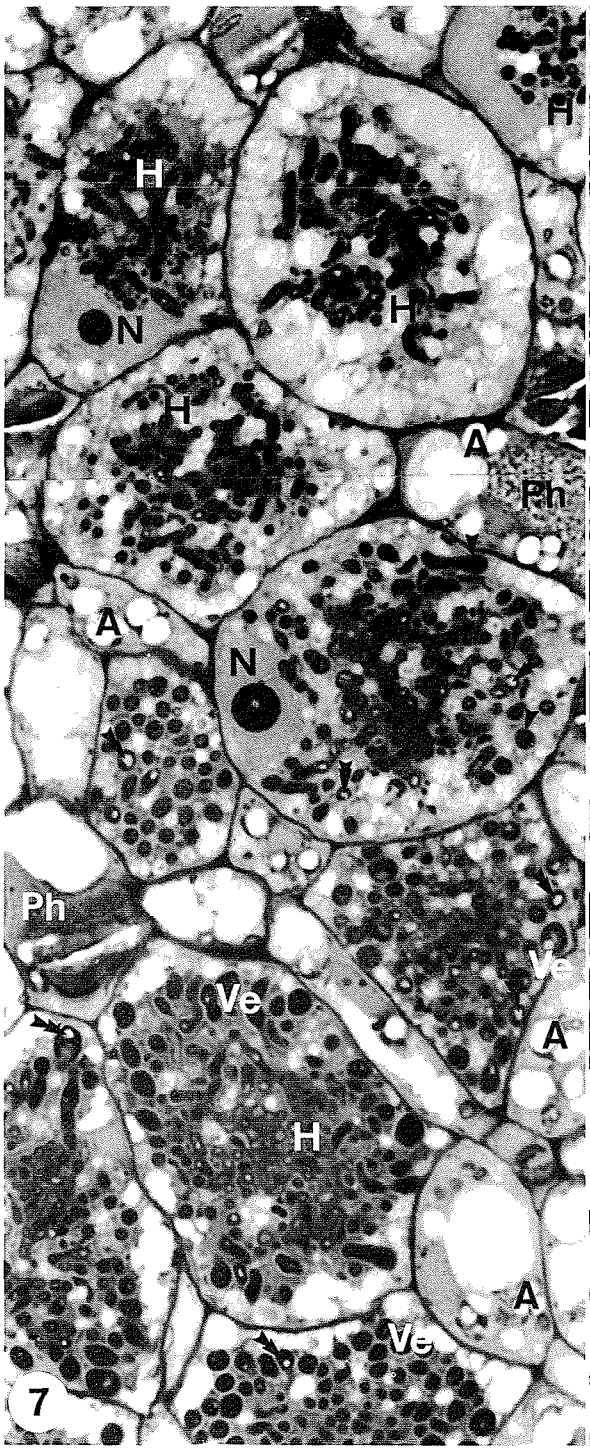


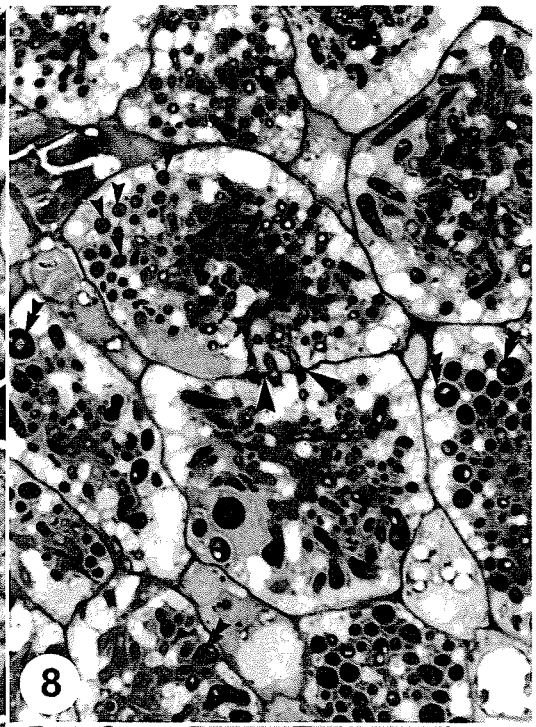


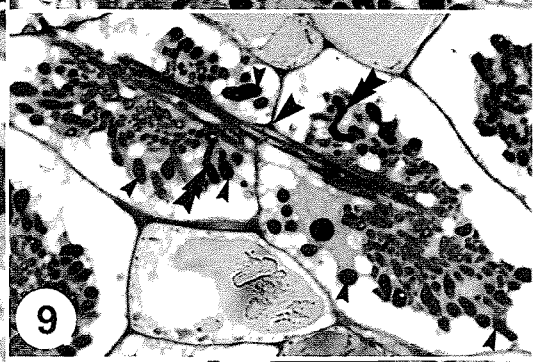


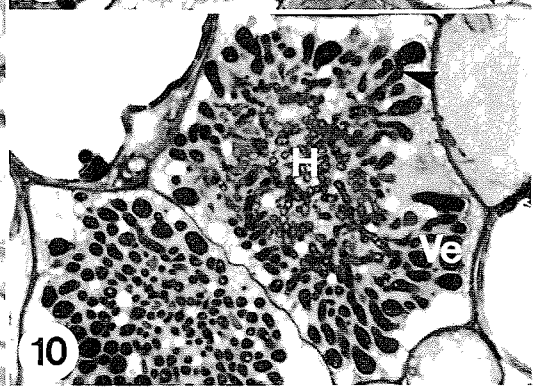

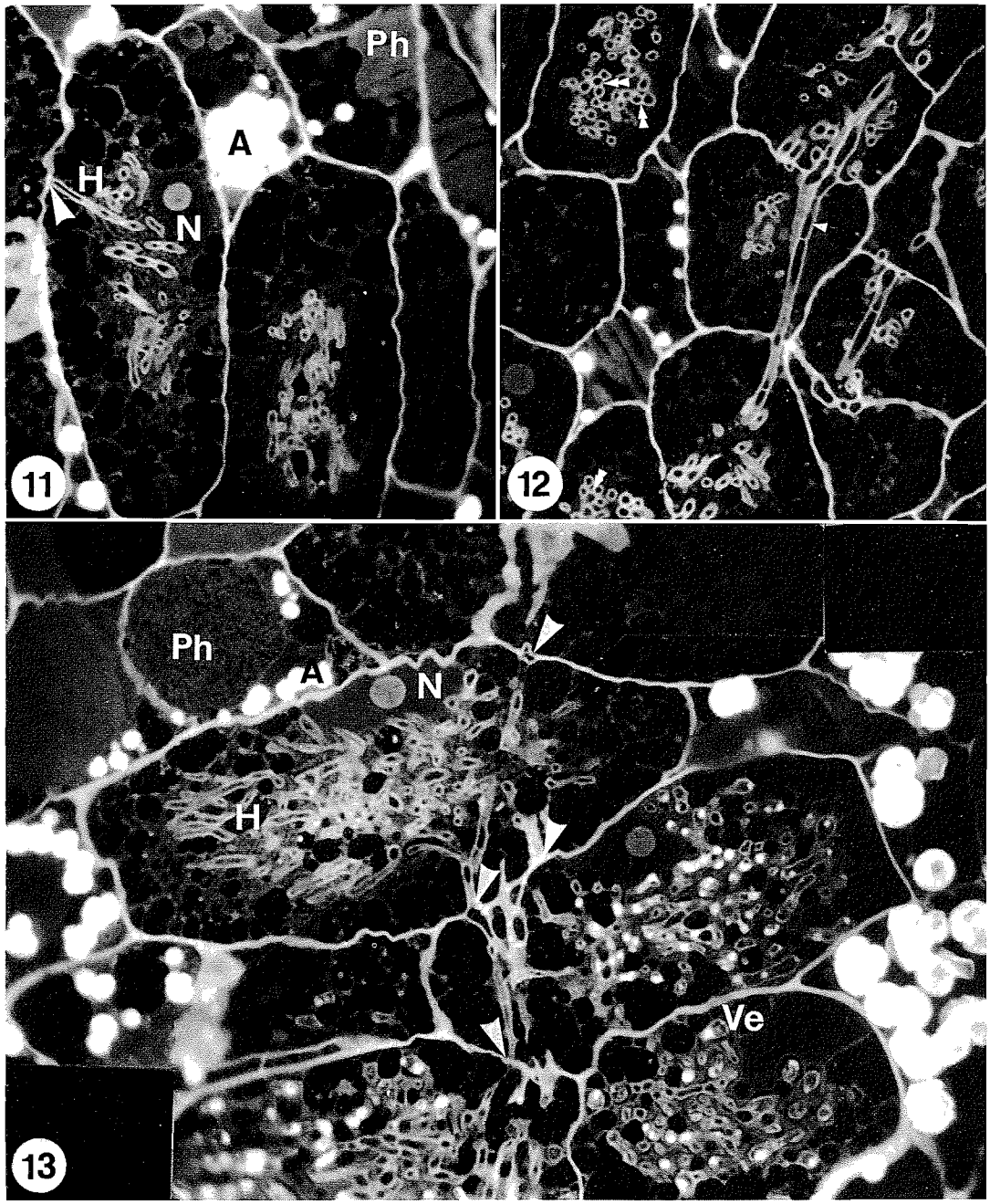


FIG. 11. Fluorescence micrograph of infected cells showing hyphae (H) penetrating central area of cytoplasm near the nucleus (N). All polysaccharides appear bright by this method. Note continuity of hyphal boundary and cell wall (arrow) and presence of phenolics (Ph) and large amyloplasts (A) in uninfected cells. × 1400. FIG. 12. Fluorescence micrograph of infected cells showing a hypha traversing (single arrows) a host cell and the fusion of hyphal capsules into a continuous structure (double arrows). × 1380. FIG. 13. Fluorescence micrograph montage of infected cells in which the endophyte is undergoing the transition from hyphal (H) to vesicular (Ve) form. Note close appression of endophyte to host nucleus (N), penetration (arrows) of hyphae through host cell wall, and phenolic (Ph) deposits and amyloplasts (A) in the neighboring uninfected cells. × 1400.

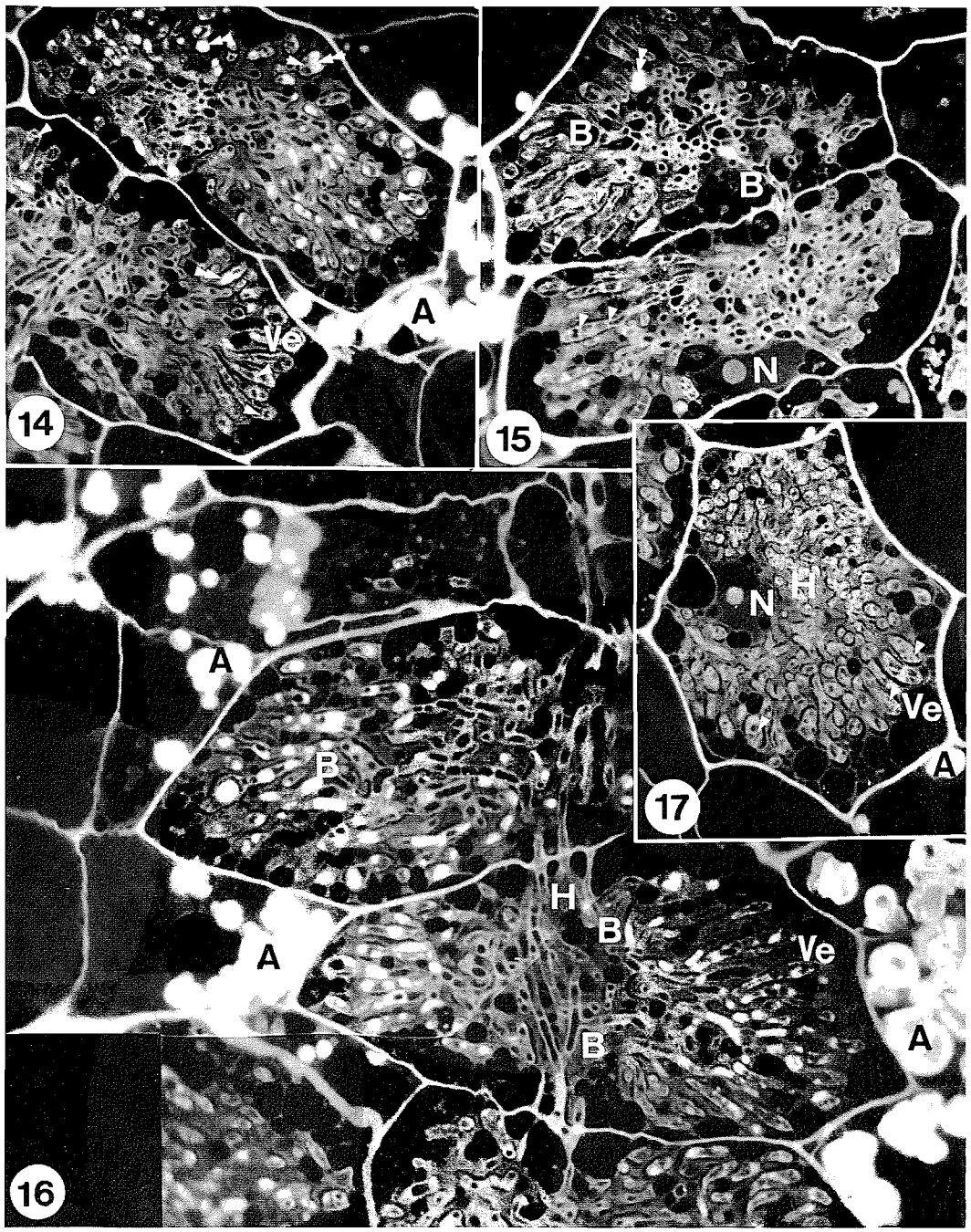


FIG. 14. Fluorescence micrograph of infected cells containing endophyte showing two stages of vesicle development. Upper cell contains vesicles with a few septa (small single arrows) and numerous PAS-positive deposits (small double arrows) while vesicles in lower cell have more septa and few PAS-positive inclusions. × 1220. FIG. 15. Fluorescence micrograph of infected cells containing endophyte with numerous septa (single small arrows) in the vesicles (Ve) and a few PAS-positive inclusions (double small arrows). Also shown is branched configuration of hypha (B). × 1220. FIG. 16. Fluorescence micrograph montage of infected cells with endophyte vesicles (Ve) in early stage of development and containing numerous PAS-positive inclusions. Note branching (B) of hypha and the abundance of amyloplasts (A) in the neighboring uninfected cells. ×1400. FIG. 17. Fluorescence micrograph of an infected cell containing endophyte with mature septate (arrows) vesicles (Ve) at the cell periphery, hyphae (H) in the centre of the cell, and no PAS-positive inclusions. × 1220.

profiles of vesicular RER are present but free ribosomes are abundant. The amyloplasts and proplastids appear to degenerate and become very electron dense (Figs. 40, 41*a*, and 45).

The vesicles of the endophyte are surrounded by capsule which is continuous with the material encapsulating the hyphae (Figs. 40, 41*a*, 44*a*–45). The capsule surrounding the vesicles is PAS-positive (Figs. 15 and 17) and reacts positively in the Thiery reaction (Figs. 42*a*, 42*b*, 43, 44*a*, 44*c*, and 45). However, a void space, presumably due to shrinkage during fixation and dehydration (Lalonde *et al.* 1976), occurs between the vesicle wall and capsule (Figs. 44*b* and 44*c*).

Senescence of the infected cells was not studied but older portions of nodules were sectioned in an attempt to find granulae similar to those reported in *Alnus* (Van Dijk and Mercus 1976) and other genera (Gardner 1976). No such structures were observed in the *Comptonia* nodule material examined.

## Discussion

The symbiotic association between a soil actinomycete and certain nonleguminous plants results in the development of root nodules. Profound structural and physiological changes occur in the roots following a series of complex interactions between the prokaryotic endophyte which contains the genetic information for nitrogenase (Skeffington and Stewart 1976) and the eukaryotic host organism which presumably contains most of the genetic information for nodule morphogenesis. It is apparent that both symbiotic partners influence the development of these complex nodular structures. The invasion of the endophyte, via a root hair into the root cortex, triggers mitotic activity in cortical cells, resulting in the formation of a prenodule (Callaham and Torrey 1977). Subsequent mitotic activity at numerous sites results in the formation of several to many primary nodule primordia which in turn give rise to other nodule lobes, resulting in the development of the mature multilobed nodule (Callaham and Torrey 1977; Bowes *et al.* 1977). The endophyte is restricted by unknown chemical or physiological factors to the middle layers of the nodule cortex and does not invade the nodule meristem. Presumably, the control of infection sites is exerted by the host. The host cells further control the infection process by encapsulating the endophyte in a polysaccharide capsule, probably pectinaceous (Lalonde and Knowles 1975*b*), which is surrounded by the host plasma membrane. Studies of freeze-etched preparations from *Alnus crispa* have established the similarity between the

FIG. 18. SEM of *Comptonia* cell wall (CW) of an infected cell with encapsulated hyphae (EH) growing on surface, broken endophyte hyphae (BEH), and perforations (Pr) penetrating the cell wall. The perforations and the encapsulated hyphae have similar diameters. The hyphae do not distort the wall surface near the penetration. The growing ends of the encapsulated hyphae are pointed (large arrows) and small protrusions (small arrows) of wall may be sites of incomplete penetration by the endophyte. × 3840. FIG. 19. SEM of *Comptonia* cell wall of an infected cell perforated by many broken encapsulated hyphae (BEH). Capsule material surrounding each individual hypha appears to have fused into one interconnected structure (arrows). The cell wall is not distorted near the sites of penetration. × 5000. FIG. 20. SEM of *Comptonia* cell wall penetrated by several broken encapsulated hyphae. A broken hyphae (BEH) is next to its perforation site (large arrow) in the host cell wall. The small protrusions (small arrows) may be sites of endophyte penetration. × 7700. FIG. 21. SEM of an infected cell containing numerous hyphae (H). The growing ends (single small arrows) of the hyphae are tapered and the hyphae bear spherical structures (small double arrows) which are the presumptive sites of branching. Hyphae have penetrated (large arrows) the host cell wall. Note plate-like appearance of fused capsule material (double large arrows). × 1950. FIG. 22. SEM of an infected cell illustrating the growing ends (single arrows) of the hyphae and the lateral bulges (double arrows) which are presumptive branch primordia. × 2600. FIG. 23. SEM of an infected cell containing large number of endophyte hyphae prior to vesicle formation. × 1300.

FIG. 24. Transmission electron micrograph (TEM) of uninfected cells located near the nodule lobe meristem. The cells contain amyloplasts (A) with starch grains (S) near the nucleus (N). Vacuoles containing phenolic deposits (Ph) commonly cuase tearing (T) during sectioning. Some vacuoles (*) lack phenolics. × 10440. FIG. 25. TEM of an uninfected cell in metaphase of mitosis located near the nodule lobe meristem. The vacuole contains large amounts of phenolics (Ph) which have been torn (T) in the sectioning process. × 7060. FIG. 26(*a*). TEM illustrating a nodule meristem cell in telophase. Numerous amyloplasts (A), mitochondria (M) and vacuoles (V), a cell plate (CP), microtubules (arrows) of the spindle apparatus, newly forming nuclei (N), branched plasmodesmata (Pd), and a large intercellular space (IS) are present. × 9160. (*b*) Higher magnification of a portion of Fig. 26*a* showing an amyloplast containing two large starch (S) grains. × 18 220. (*c*) Higher magnification of a portion of Fig. 26*a* showing elaborately branched plasmodesmata with a middle sinus (arrows). × 22 080.

FIG. 27. (*a*) TEM of newly infected cells containing numerous hyphae (H), a nucleus (N) with a prominent nucleolus (Nu), many small vacuoles (V) some of which contain phenolics (Ph), and a few amyloplasts (A). × 3140. (*b*) Higher magnification of area outlined in Fig. 27*a*. Shown are hyphae (H) growing in the middle lamella between adjacent cell walls (CW) and protruding into host cytoplasm. The hyphae are surrounded by a polysaccharide capsule (single small arrows) which is bounded by the host plasma membrane (double small arrows). Numerous profiles of vesiculate rough endoplasmic reticulum (large arrows) containing an electron-dense fibrillar matrix are present. × 11 800.

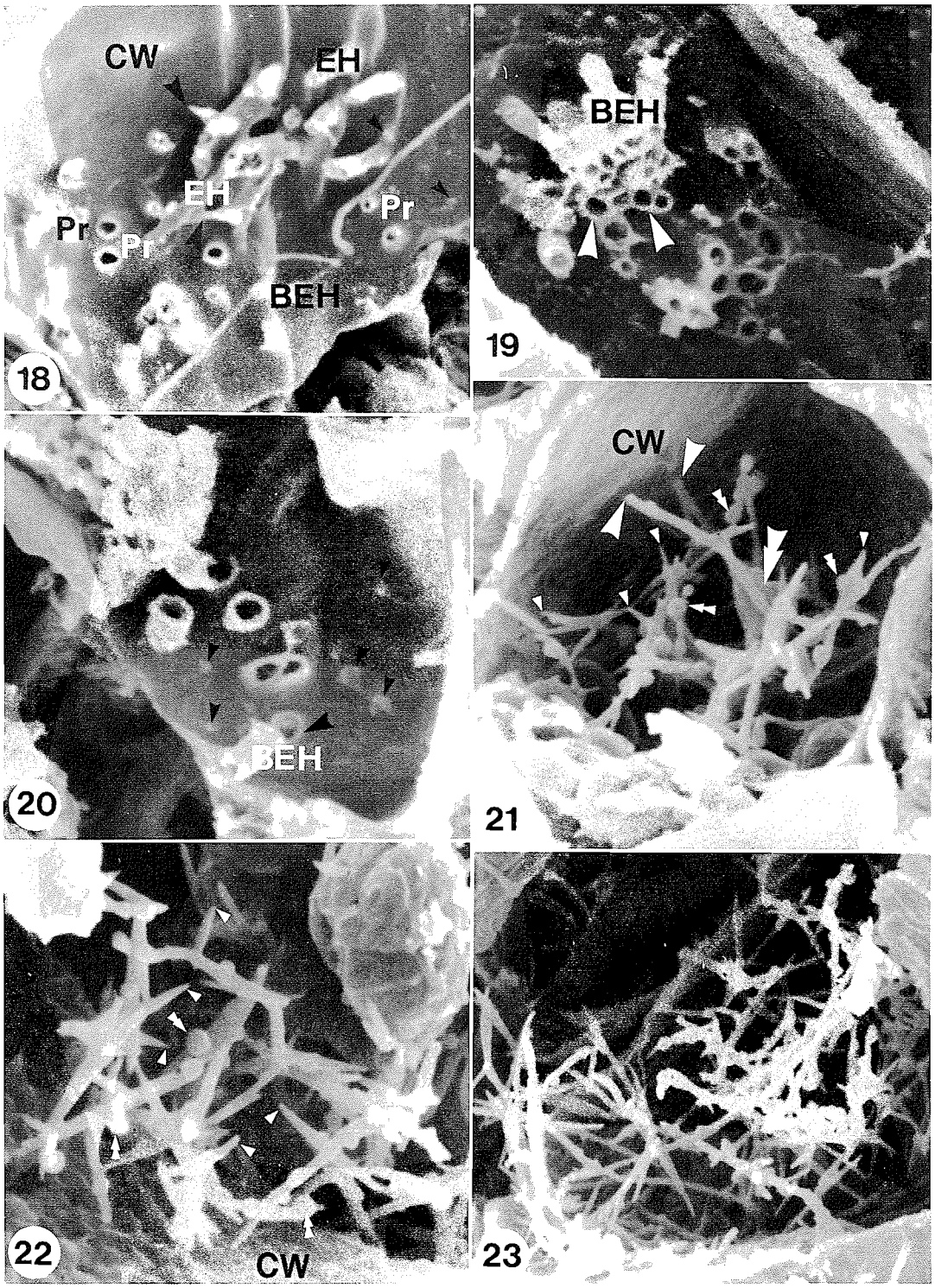

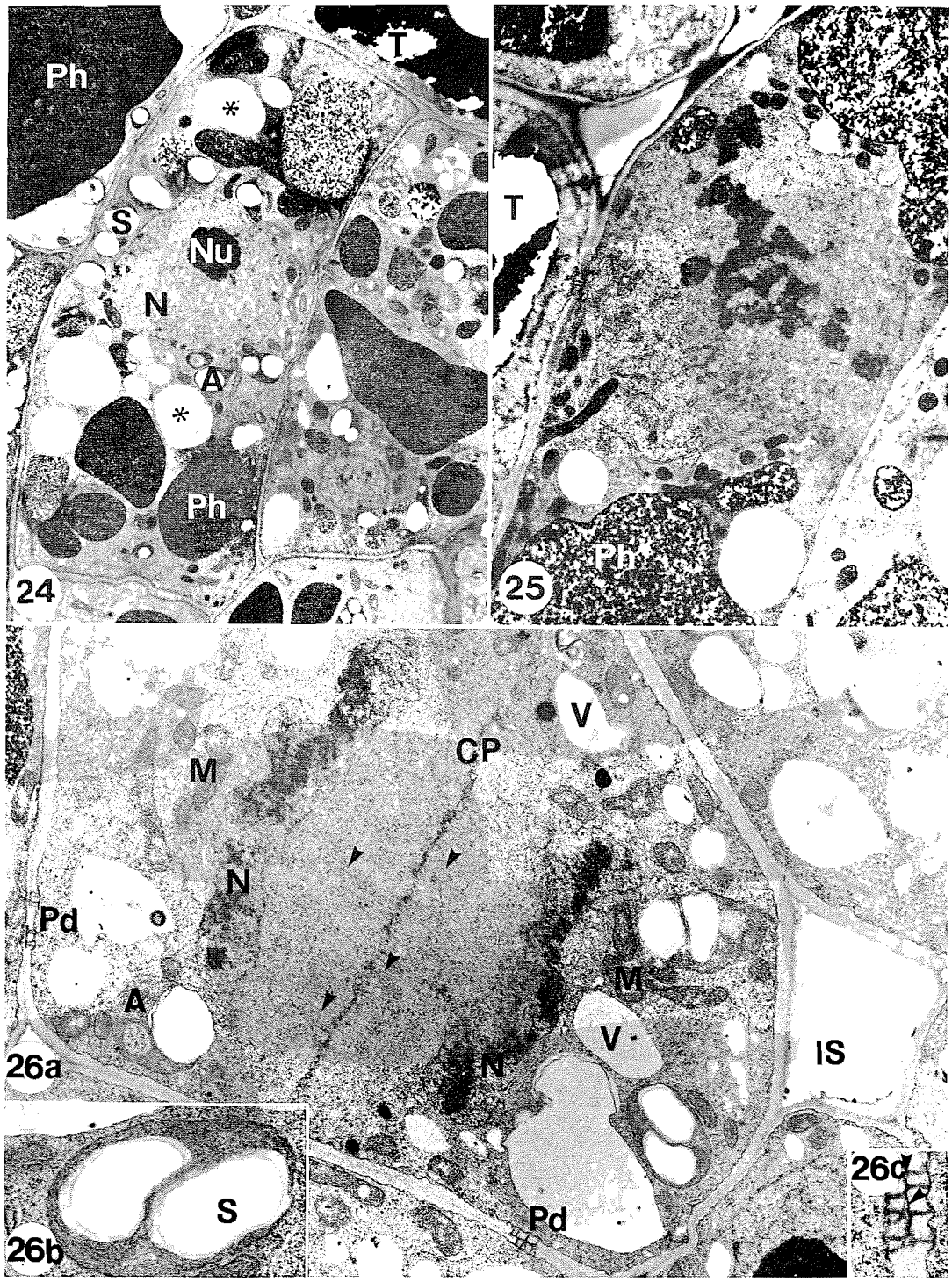

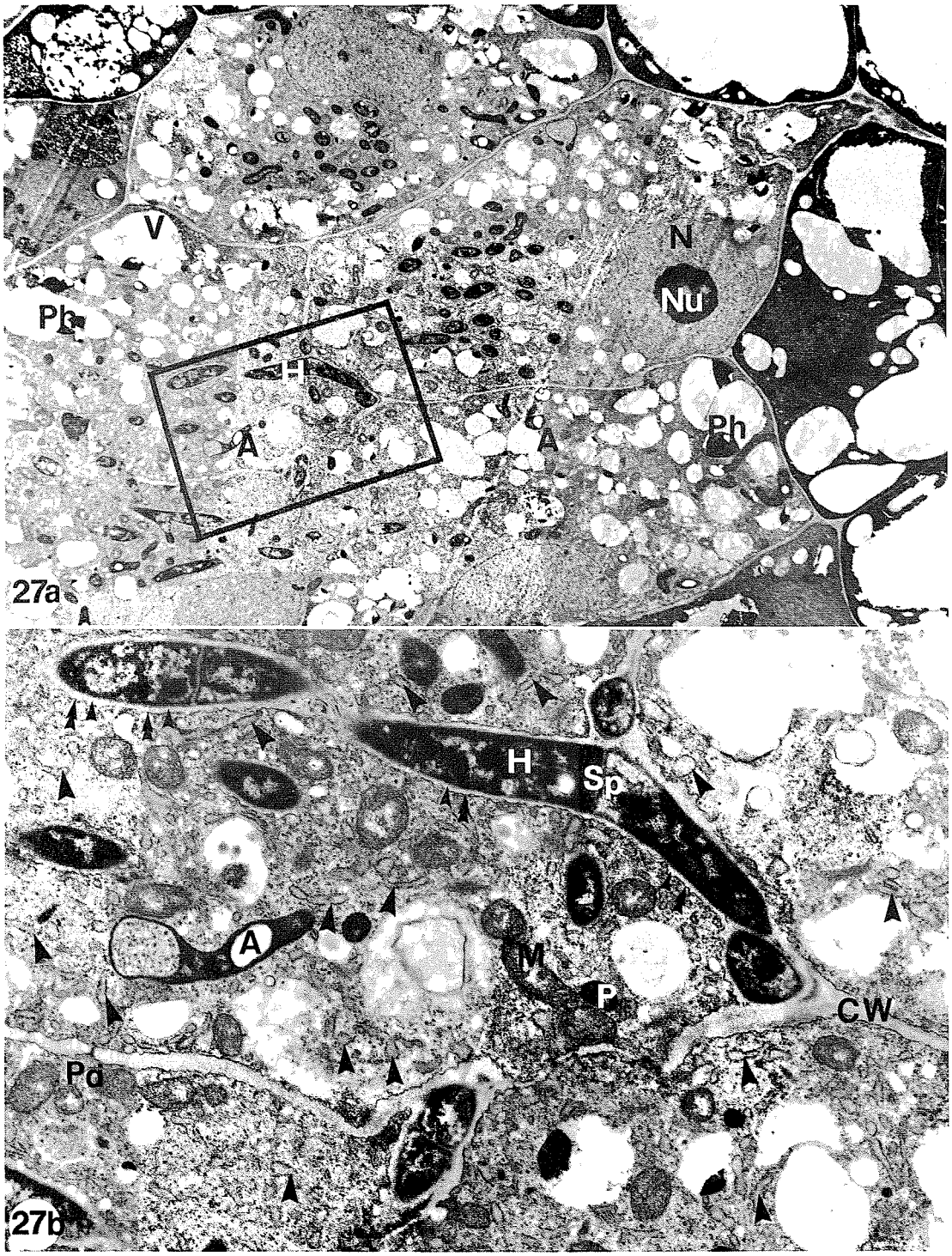

host cell plasma membrane and the membrane surrounding the endophyte (Lalonde and Devoe 1976).

*Invasion of the Host Cells by the Endophyte*

One of the intriguing aspects of nodule morphogenesis is the intracellular establishment of the endophyte without damage or death of the host cells. The present study suggests that the endophyte of *Comptonia* nodules passes through the host cell wall by means of localized chemical degradation which allows penetration of the hyphae. Chemical changes in the cell wall may also be involved to some degree in the formation of the capsule. Root nodules of *Alnus glutinosa* are the sites of high pectolytic activity (Lalonde 1977). SEM observations of *Alnus crispa* (Lalonde and Devoe 1975) and those made on *Comptonia* clearly demonstrate the presence of regular perforations of the proper dimensions to be occupied by the endophyte. It is equally clear from TEM and SEM that the contours of the host cell wall are not disturbed when the endophyte penetrates the wall. This observation agrees with previous suggestions (Silver 1964; Lalonde and Knowles 1975*a*) that the penetration of the endophyte is not due to mechanical forces. The occasional occurrence of thin regions of host cell wall presumably results from endophyte-secreted enzymes which degrade the wall. It is possible that the dense membrane-bound substance we observed (Figs. 31*a*, 31*b*, and 31*c*) is involved in the repolymerization of the degradation products into the capsule.

*Encapsulation of the Endophyte*

The similarity between the infection thread of leguminous nodules (Dart 1975; Newcomb 1976) and the capsule of the endophyte in nodules appears to be a superficial one. The current interpretation of the rhizobial infection thread is that it is formed as an invagination of the host cell wall. Although the presence of cellulose in the wall of the infection thread suggests that it is derived from the host cell wall, it is not clear how the latter can become so extended (Newcomb 1976). In addition, rhizobia are distributed to host cells via the thread and rhizobia multiply within the thread. In contrast, the actinomycete endophyte grows into each host cell subjected to infection and is always surrounded by the capsule. Thus, endophyte and capsule growth occur at similar rates. The capsule is not an invagination of the host cell wall; rather, it is composed of pectin and contains no cellulose (Lalonde and Knowles 1975*b*).

The source of the components for the capsule is uncertain. In young nodules of *Comptonia* a marked proliferation of RER occurs in newly infected cells. The RER is located near the growing hyphae and often appears to fuse with the capsule (Figs. 27*b*, 29, 32, 33, and 34). Significantly, very little RER is present after hyphal growth has ceased (Figs. 38*b*, 40, and 41*a*). While the capsule reacts positively in the Thiery reaction, the fibrillar material within the RER does not. Since the Thiery reaction does not detect sugars with β-1,3 linkage the possible involvement of RER in capsule forma-

FIG. 28. TEM showing two hyphae (H) in longitudinal section penetrating the cell wall (CW) with little distortion and another hypha cut in transection growing in the cell wall and distorting the shape of the wall. Note the capsule (C) surrounding the endophyte, vesiculate rough endoplasmic reticulum (arrows) in process of fusing with capsule, transverse septum (Sp) in the hypha, electron-dense granules (G), and plasmodesmata (Pd) in the host cell wall. × 29 770. FIG. 29. TEM showing hyphae (H) penetrating the host cell wall (CW), a multivesicular body (MVB) containing many smaller vesicles, numerous small vesicles (large arrows) that may be about to fuse with host plasma membrane (double small arrows) surrounding capsule (C), some vesicles that have already fused (single small arrows) with host plasma membrane, and profiles of vesicular rough endoplasmic reticulum (RER) containing a fibrillar matrix. × 31 570. FIG. 30. TEM showing hypha (H) growing between adjacent cell walls (CW) and branching in two directions into cells. Plasmodesmata (single arrows) and a transverse septum (double arrows) are also illustrated. × 11 140.

FIG. 31. (*a*) TEM showing portions of two infected cells in which the host cell wall (CW) is thinner at the centre than at the edges of the cell. One area (arrow) of the wall appears to be absent, possibly due to degradation associated with penetration of the endophyte. Several areas of membrane-bound electron-dense substance (DS) are located adjacent to the host cell wall and capsule. × 13 310. (*b*) Higher magnification of portion outlined in Fig. 31*a*, demonstrating that membrane-bound, electron-dense substance (DS) is continuous (arrows) with both the host cell wall and the capsule (C). × 28 230. (*c*) Higher magnification of outlined portion of Fig. 31*b* illustrating fibrillar material (arrows) near degraded portion of cell wall. × 67 250.

FIG. 32. TEM of an infected cell showing hyphae (H) (sectioned transversely) surrounded by a capsule (C). Numerous profiles of vesiculate rough endoplasmic reticulum (RER) containing a fibrillar material are present and often appear to fuse (large arrows) with the capsule. Also shown are a few microtubules (small arrows). × 29 450. FIG. 33. TEM of two hyphae surrounded by a capsule (C) which is bounded by the host plasma membrane (double large arrows). Endophyte is bounded by its plasma membrane (large single arrows) and two layers of wall, the outer layer (small single arrows) being the denser of the two. Internally, the hyphae show an outer dense cytoplasm containing many ribosomes, a nucloid area with fibrillar (F) material, and many small vesicles (*). Also shown is a microtubule (double small arrow) and a vesicle (triple small arrows) that may be fusing with the capsule. × 45 950. FIG. 34. TEM of a newly infected cell showing hyphae (H) sectioned obliquely and longitudinally, numerous profiles of rough endoplasmic reticulum (arrows), and a nucleus (N) containing a nucleolus (Nu) and dispersed heterochromatin (HC). × 7530.

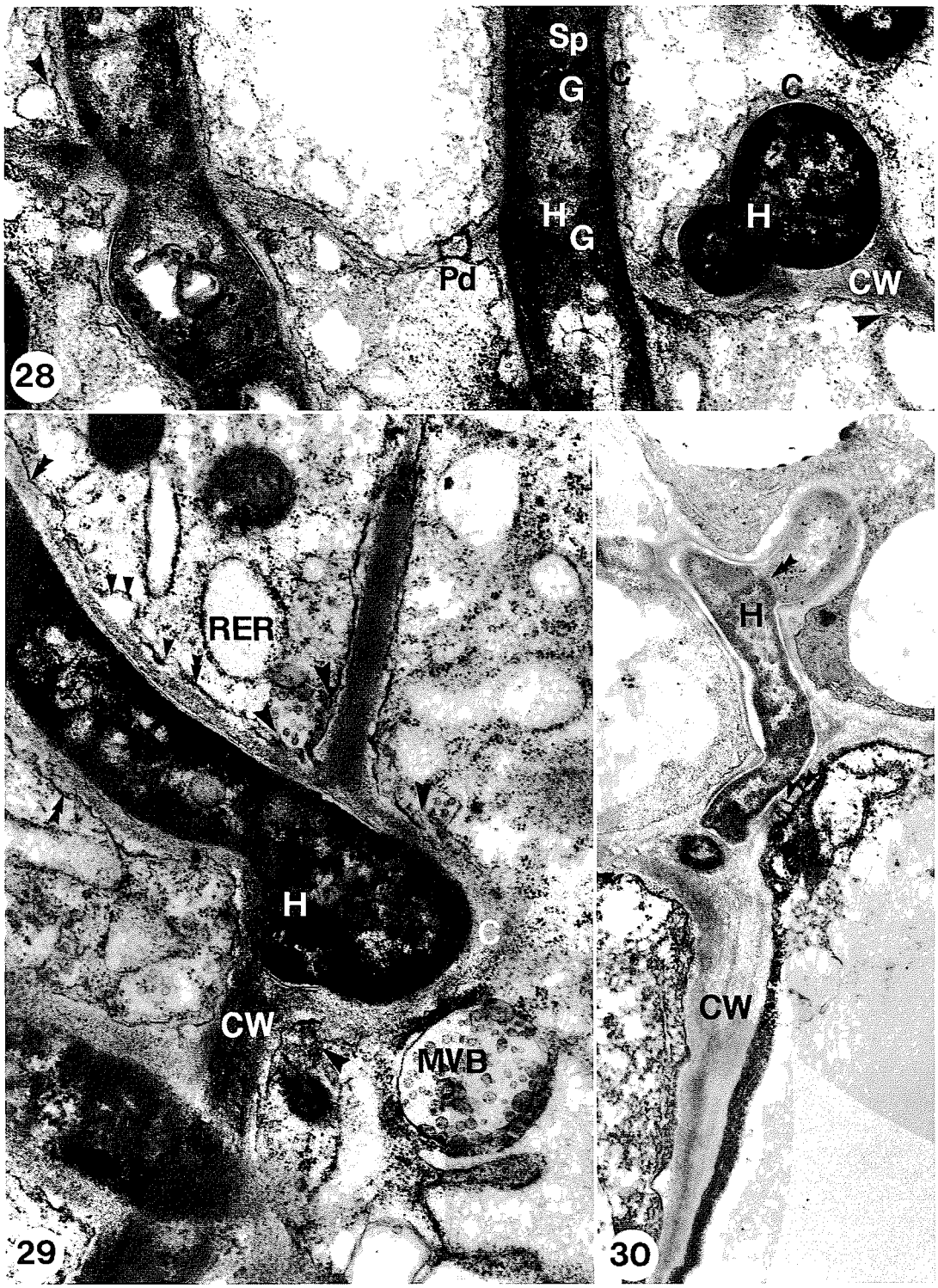

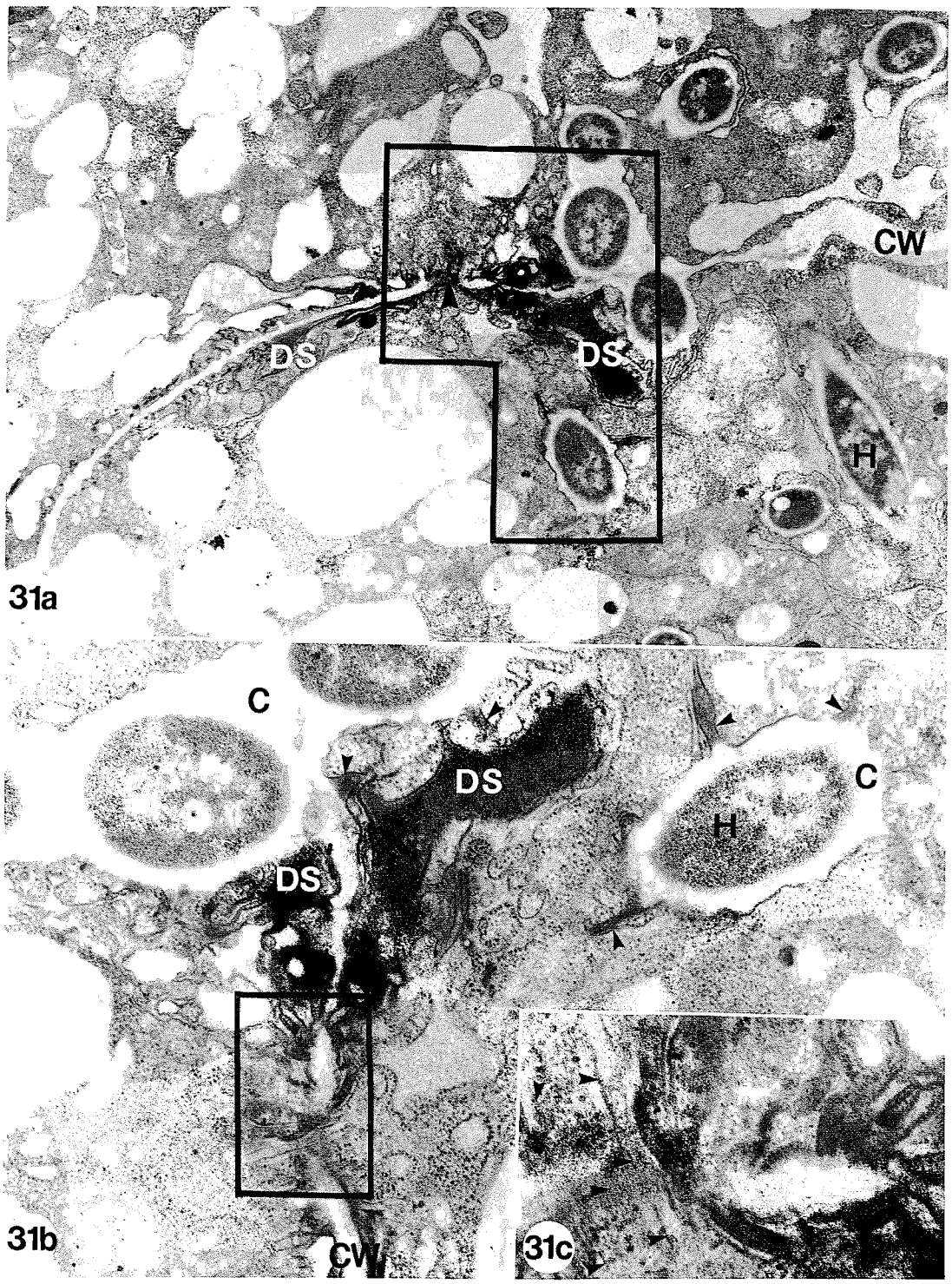

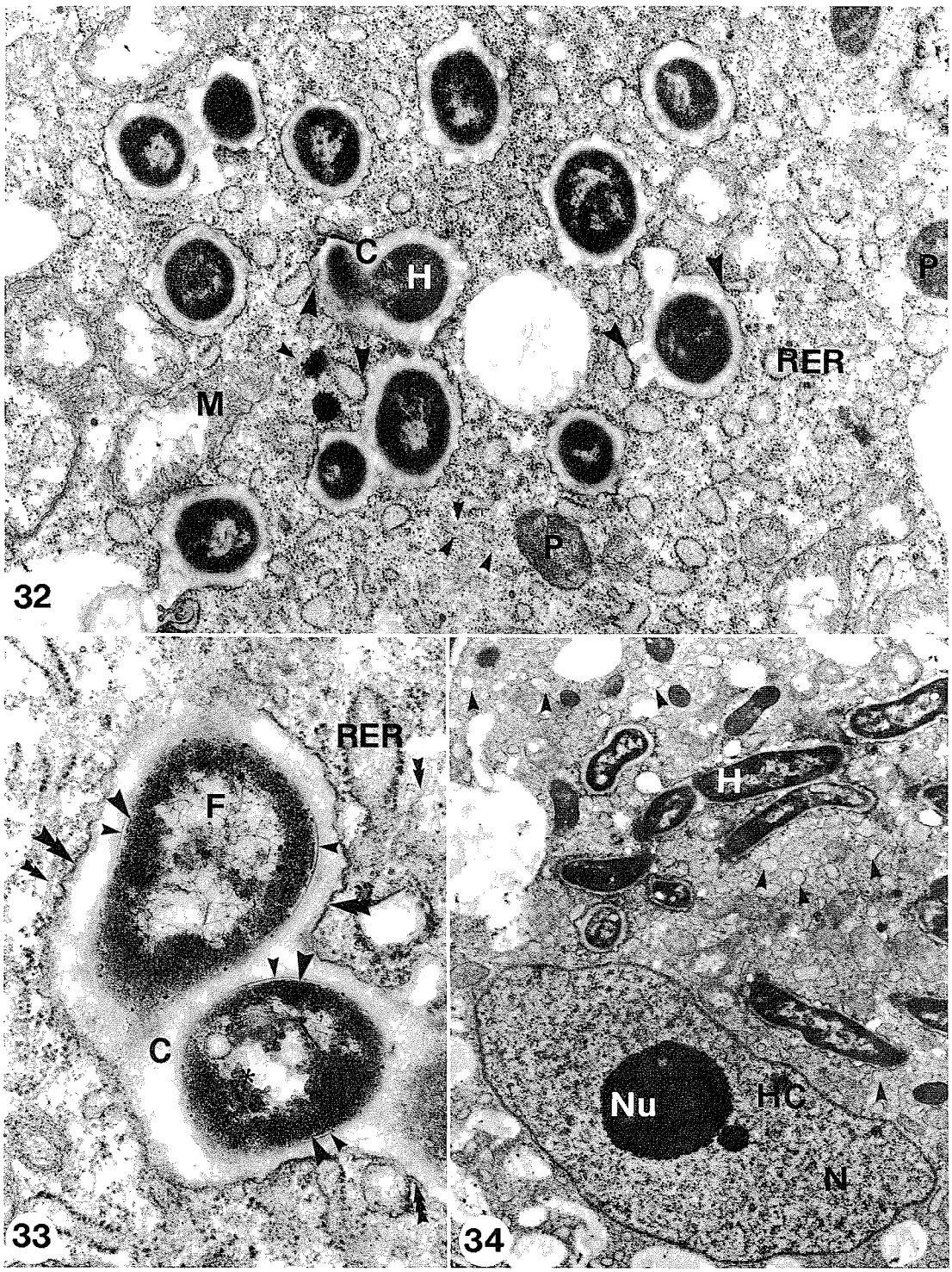

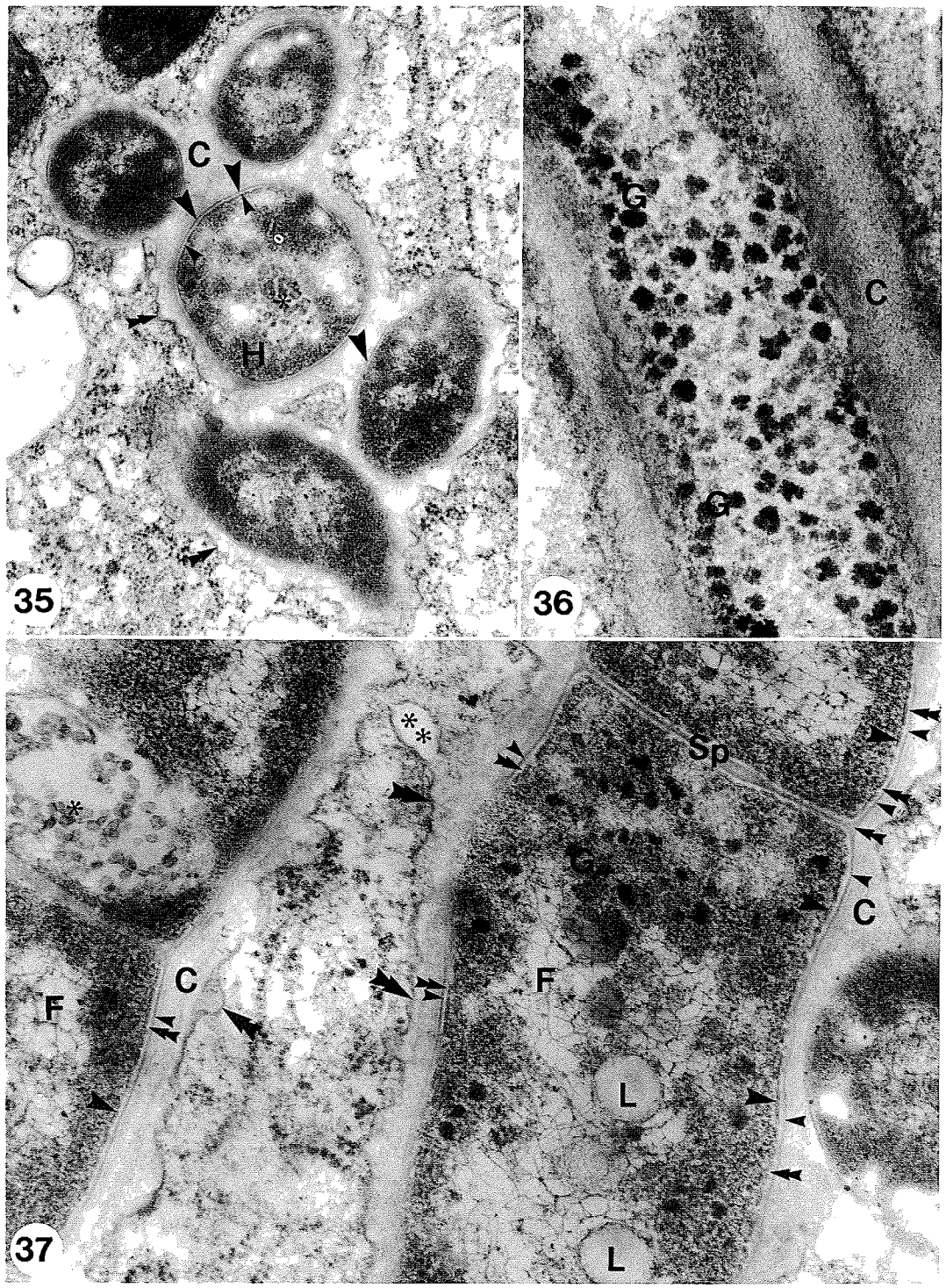


FIG. 35. TEM showing continuity of capsule (C) which surrounds five hyphae (H) of the endophyte. Note the small vesicles (*) within the endophyte, the plasma membranes of the endophyte (single small arrows) and of the host (double small arrows), and the two layers of the endophyte cell wall (large arrows). × 34 360. FIG. 36. TEM of endophyte showing numerous electron-dense granules (G) and capsule (C). × 71 070. FIG. 37. TEM of endophyte illustrating a cross septum (Sp), the outer (single small arrows) and inner (double small arrows) layers of the endophyte cell wall, the plasma membranes of the endophyte (single large arrows) and host (double large arrows), and fibrillar (F), lipid (L), and vesicular (*) inclusions in the endophyte. Wall material may be fusing (**) with the capsule. × 57 310.

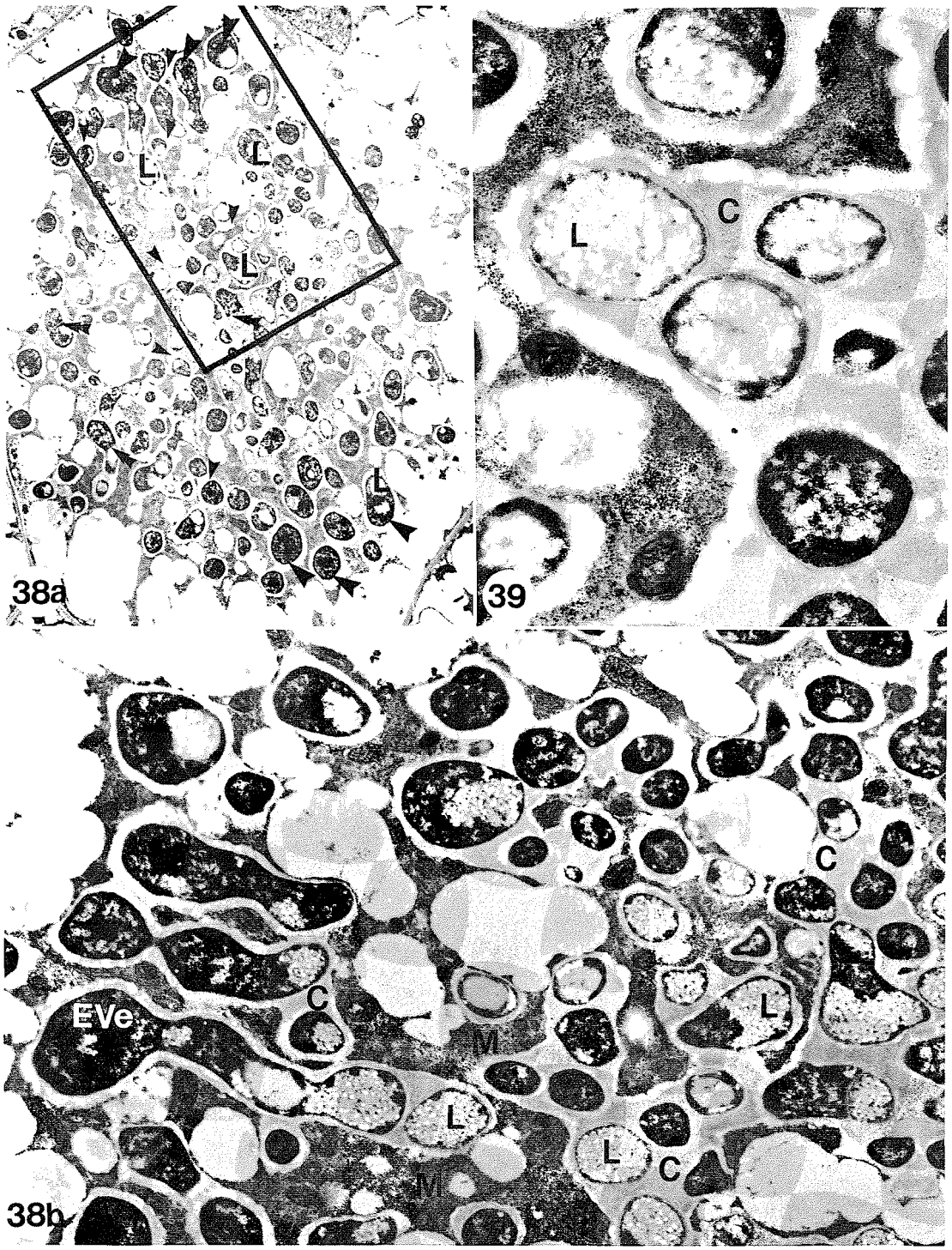


FIG. 38. (*a*) TEM of infected cell in which the ends of the hyphae have become swollen (large arrows). The endophyte contains numerous electron-opaque inclusions that may be lipid (L). The capsule (small arrows) is more extensive in the centre of the cell than at the periphery of the cell near the hyphal tips. A few septa (double small arrows) are present in the hyphae. × 4000. (*b*) Higher magnification of outlined area in Fig. 38*a* showing the swollen hyphal tips or early vesicles (EVe), the continuity of the capsule (C) around the endophyte, the numerous electron-opaque, lipid-like inclusions (L), and many mitochondria (M). × 6960. FIG. 39. TEM of a cell similar to that shown in Fig. 38*a* in which the hyphae, located in the central part of the cell, contain numerous lipid-like electron-opaque inclusions (L). × 24 170.

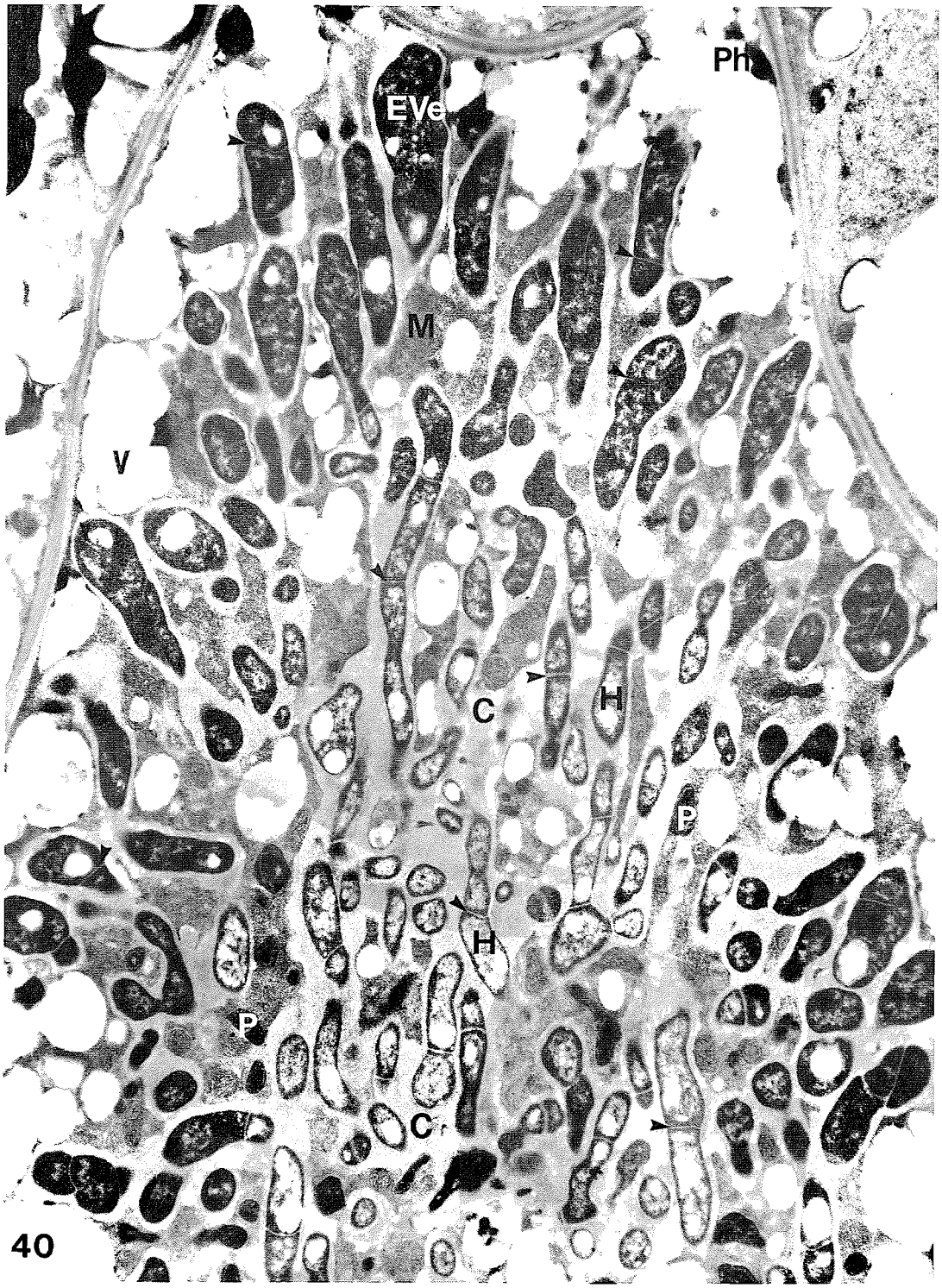


FIG. 40. TEM of an infected cell containing the early vesicle stage of the endophyte. The vesicles have elongated (cf. Figs. 38*a* and 38*b*) and a few septa (single arrows) are present. Note the thickness and continuity of the capsule (C) around the endophyte. Degenerate electron-dense proplastids (P), numerous mitochondria (M), and small amounts of phenolics (Ph) are present in the vacuoles (V). × 7260.

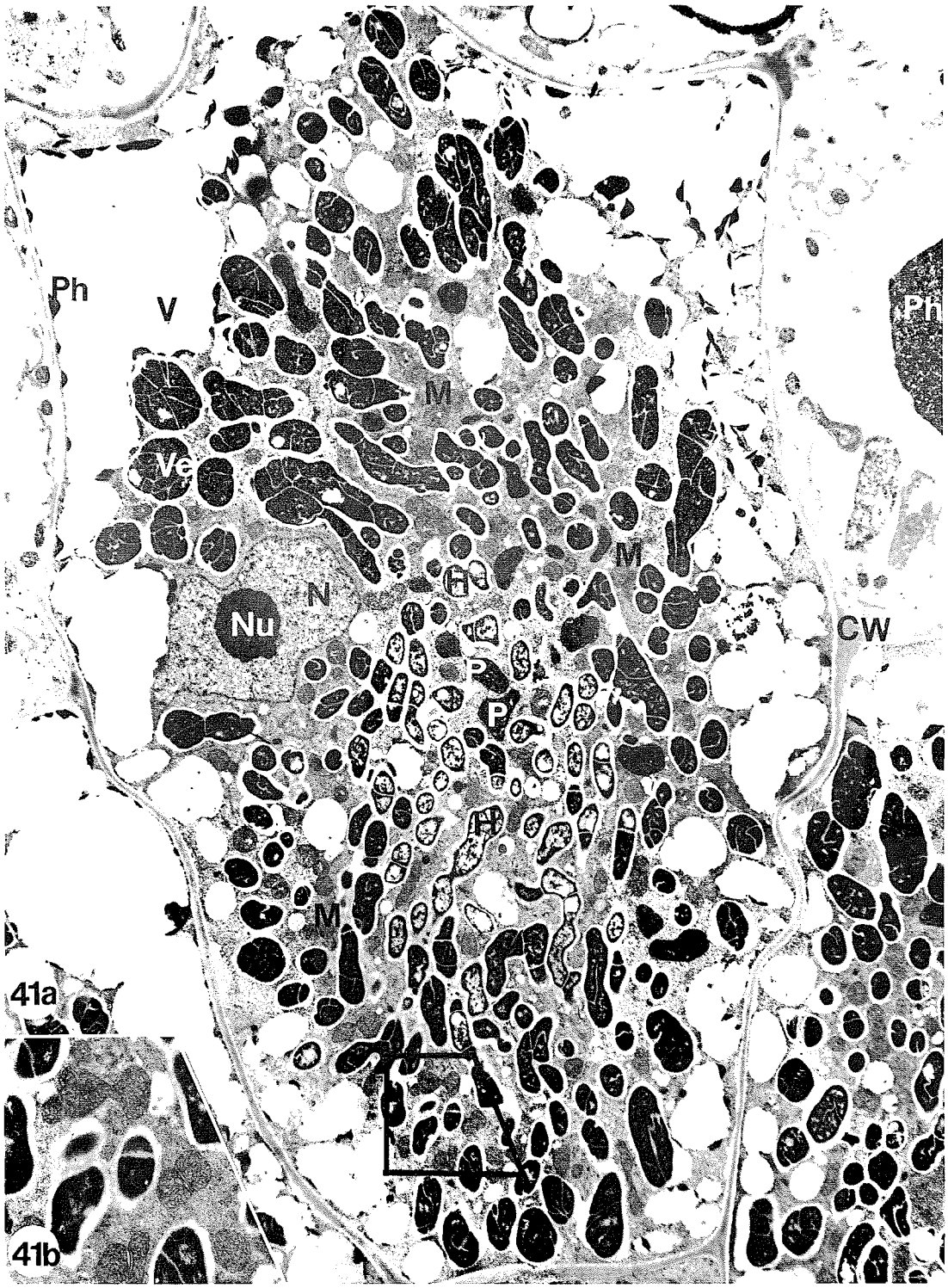


FIG. 41. (*a*) TEM of infected cell packed with developing vesicles (Ve) containing numerous complete and incomplete septa. Note convoluted shape of nucleus (N) which still has a prominent nucleolus (Nu), numerous groups of mitochondria (M), degenerate proplastids (P), and small deposits of phenolics (Ph). There is a marked difference in density between the central endophyte hyphae (H) and the terminal vesicles. × 4740. (*b*) Higher magnification of outlined area in Fig. 41*a* showing mitochondria that are possibly dividing and two pairs of joined mitochondria which may have just finished dividing. × 10 200.

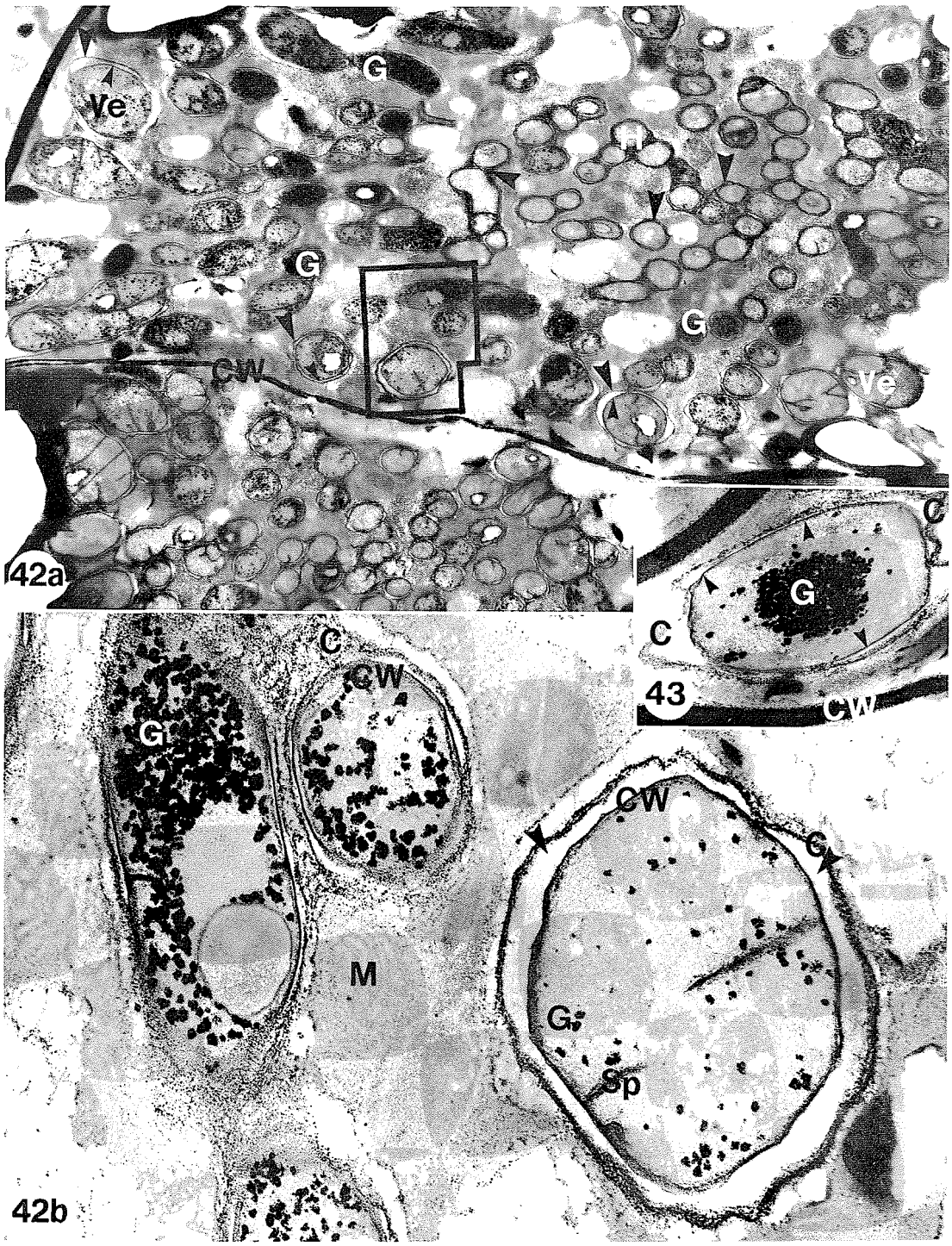


FIG. 42. (*a*) TEM of infected cells with developing vesicles (Ve) of the endophyte stained with Thiery reaction for polysaccharide which stains black. The host cell wall (CW), numerous granules (G) of the endophyte, endophyte cell walls (small arrows), and capsule (large arrows) have reacted positively × 6330. (*b*) Higher magnification of area outlined in Fig. 42*a*. demonstrating positively reacting capsule (C), granules (G) within endophyte, and cell walls (CW) and septa (Sp) of endophyte. Note void space (arrows), presumably a fixation artefact between the capsule and endophyte cell wall. × 21 040. FIG. 43. TEM section stained with Thiery reaction showing an early vesicle of the endophyte. Numerous granules (G), the endophyte cell wall (arrows), the capsule (C), and the host cell wall (CW) reacted positively Note void space between capsule and endophyte cell wall. × 37 800.

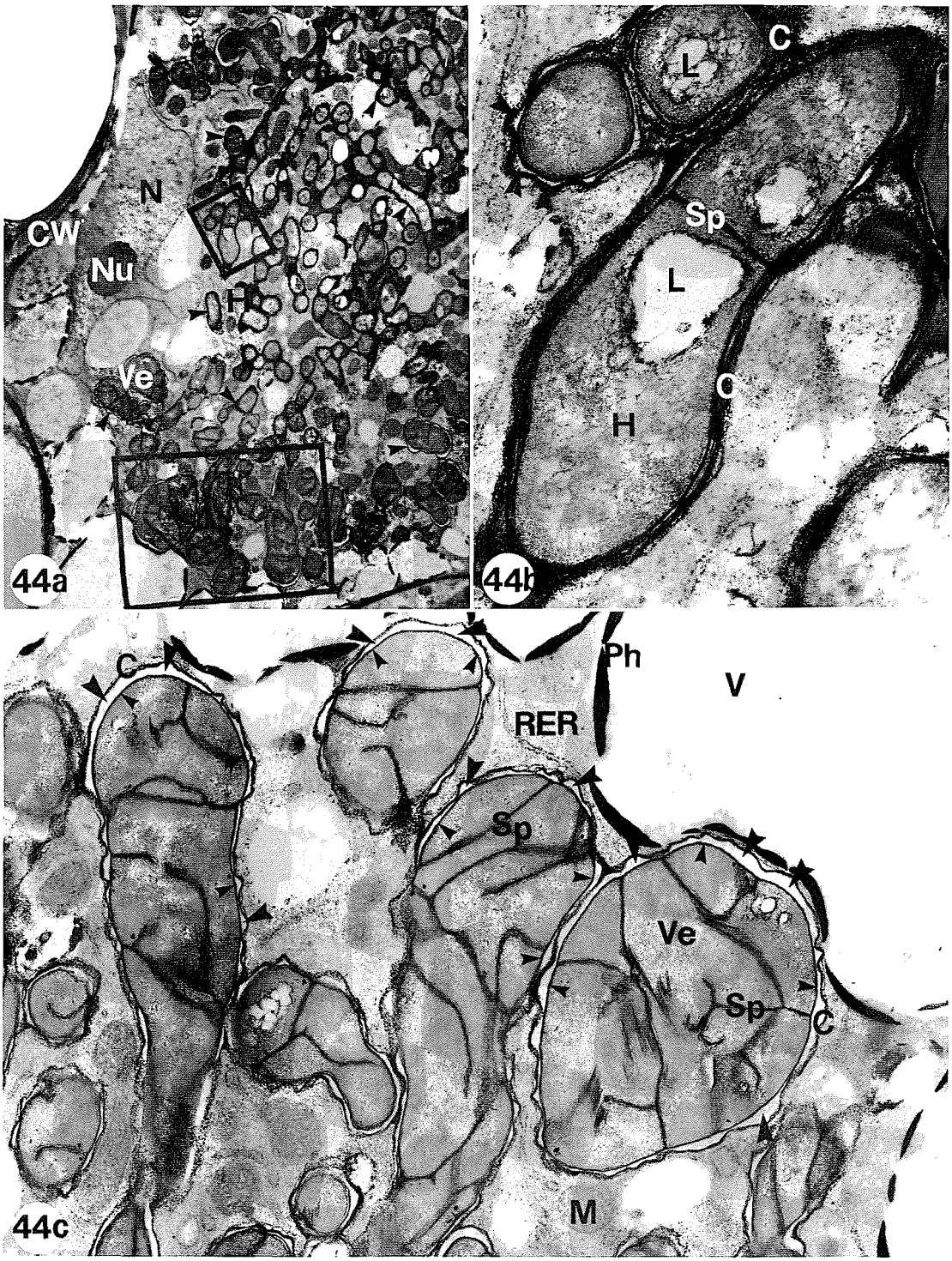


FIG. 44. (*a*) TEM of section stained with Thiery reaction showing an infected cell containing mature vesicles (Ve) of the endophyte. Note that the positive-reacting capsule (arrows) is thicker near the hyphae (H) than near the vesicles. × 3150. (*b*) Higher magnification of small area outlined in Fig. 44*a*. The capsule (C) and septum (Sp) both reacted positively. Some areas of the capsule pulled away from the endophyte cell wall, creating a small void space (arrows). A lipid-like inclusion (L) reacts negatively although material at the edge of these inclusions does react positively. × 32 160. (*c*) Higher magnification of large area outlined in Fig. 44*a*. Capsule (C), endophyte cell walls (small arrows), and septa (Sp) have reacted positively. Note void space (large arrows) due to capsule pulling away from endophyte cell wall during tissue preparation. × 16 470.

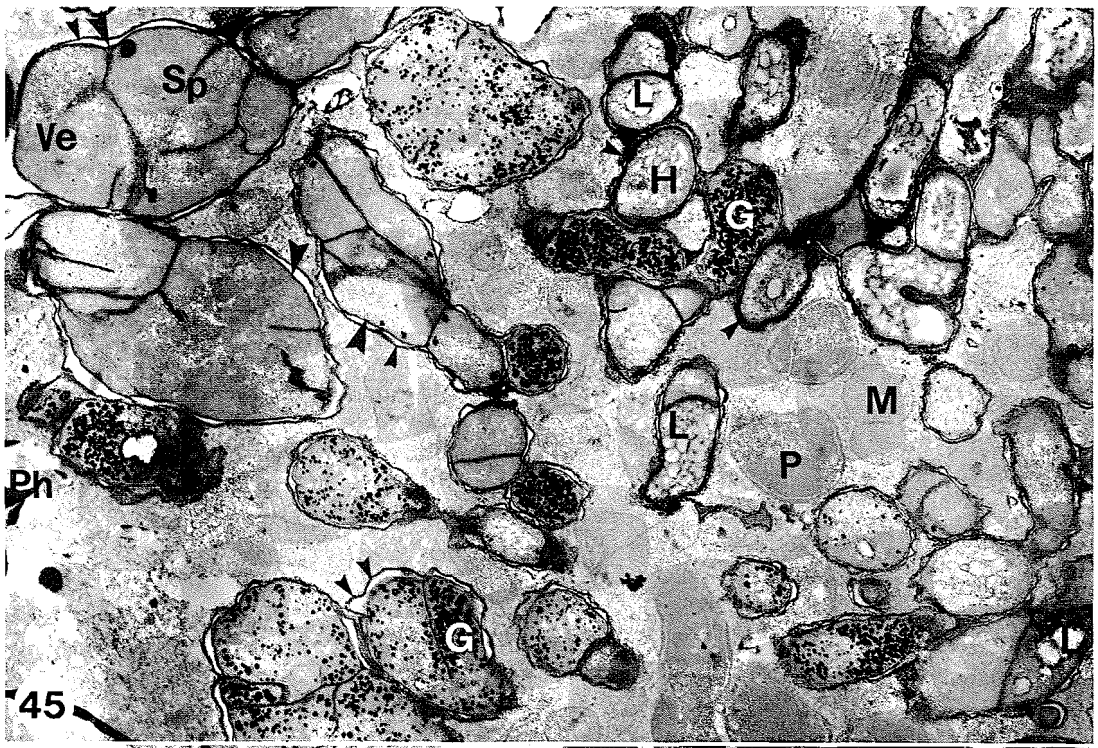


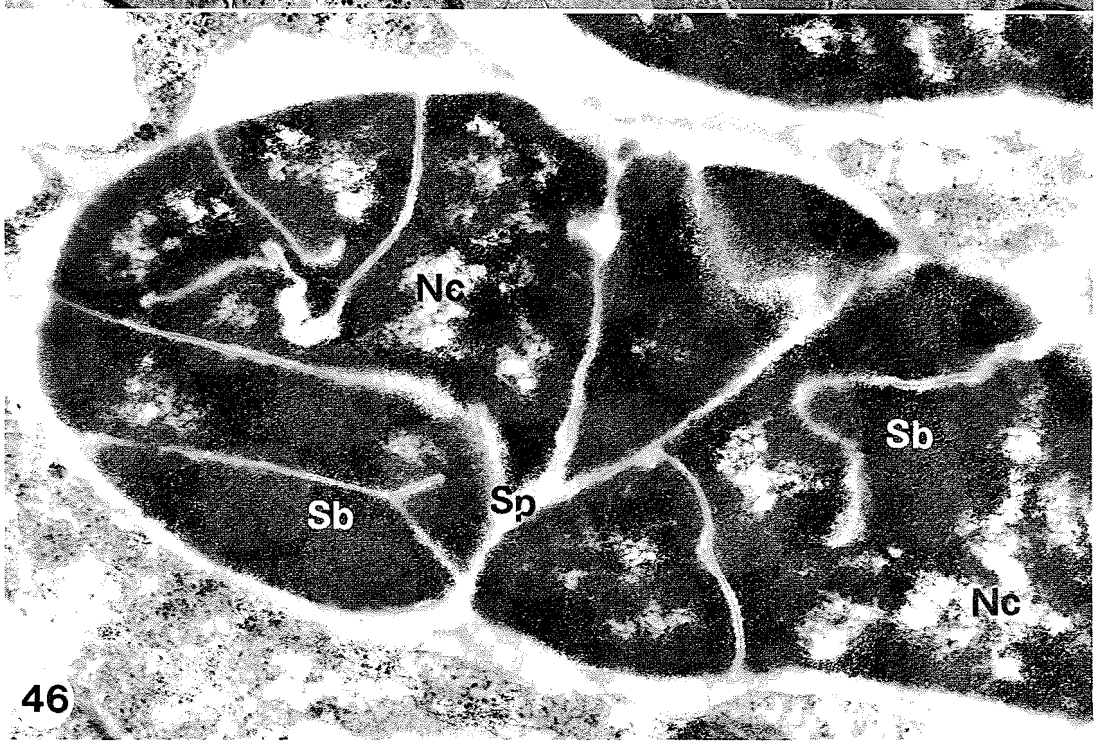


FIG. 45. TEM of Thiery-stained section illustrating positive-staining granules (G) in hyphae (H) and immature vesicles (Ve). Lipid-like (L) inclusions did not react. Positive-reacting capsule is pulled away from endophyte cell wall (large arrows). × 12 620. FIG. 46. TEM of mature vesicle showing complete and incomplete septa (Sp), striated bodies (Sb), and nucloid (Nc) areas. × 35 550.

tion cannot be ruled out. It is also possible that low-molecular-weight, soluble sugar polymers were lost during fixation and dehydration. The involvement of host organelles in the formation of the capsule in *Alnus crispa* has been suggested (Lalonde and Knowles 1975*b*). However, it should be pointed out that the endophyte could also be involved in the synthesis of the carbohydrates of the capsule. The capsule is very extensive and results in the formation of a large continuous plate-like structure in the center of infected cells (Figs. 12, 15, 21, 22, and 40). The function of the capsule is not known; presumably its presence and complete encasement of the endophyte exerts a limitation on uncontrolled proliferation of the endophyte within the host.

*Differentiation of the Infected Cell*

In addition to the proliferation of RER mentioned above, the invasion of the endophyte and its subsequent morphogenesis coincide with an increase in cell size, an increase in numbers of mitochondria, and loss of starch from the amyloplasts. The size of the nucleus and nucleolus remains stable during the morphogenesis of the endophyte; in other actinomycete-nodulated species, it has been demonstrated that the nodule meristem cells are diploid (Bond 1977). This is unlike the legume–rhizobium symbiosis in which the host nucleus often becomes polyploid (Mitchell 1965; Dart 1975). The increase in the mitochondrial population appears most obvious during the formation of septa in the vesicles; at this time mitochondria may be observed in apparent division or clumped together in groups of two or three (Figs. 41*a* and 41*b*). The amyloplasts lose their starch shortly after the invasion of the endophyte (Figs. 3–6 and 27*b*) and the proplastids are degenerate when the vesicles are maturing (Figs. 41*a* and 45). The utilization of starch and an increase in mitochondrial number may correspond with increased energy requirements for growth and nitrogen fixation. Becking (1977) claimed that in nodules of *Alnus* nitrogenase activity occurs in vesicles of the endophyte rather than in simple hyphal stages, and Akkermans (1971) showed that vesicles are sites of high reducing activity. Organelle changes in the host cells would appear to fit these proposals. Conclusive evidence for the presence of active nitrogenase only in vesicles is lacking.

*Differentiation of the Endophyte*

The formation of the vesicles occurs only after the hyphal stage of the endophyte has penetrated most of the host cytoplasm exclusive of the cell periphery, which is largely composed of numerous vacuoles (Fig. 7). Furthermore, in *Comptonia* the vesicles only develop near the cell periphery. The development of septate, club-shaped vesicles coincides with the appearance of numerous lipid-like inclusions and Thiery-positive granules within the endophyte. Most of the lipid-like substance is confined to the hyphae, but the rosette-shaped granules which appear similar to glycogen may also be present in the early stages of vesicle formation as well as in the hyphae. Only small amounts of either substance are present after the vesicles are mature. These substances may serve as substrates for growth and differentiation of the septate vesicles.

*Role of Phenolics*

The amount of phenolic substances in the vacuoles of uninfected cells in mature nodules of nonleguminous plants judged from histological staining reactions is usually large. While young nodules contain only small amounts of phenolics, old nodules may have very high levels. During the course of this study, numerous bacteria and fungi were observed on the surface of *Comptonia* nodules, but no organisms other than the endophyte were found inside the nodule. Phenolic substances could be important in preventing secondary infections of the nodules and might function to retard the feeding of animals on the nitrogen- and carbohydrate-rich nodules. Such a role has been suggested for the occurrence of phenolics in the root meristem and cap of the fern *Ophioglossum petiolatum* (Brisson *et al.* 1977).

## Acknowledgments

This study was initiated while the senior author was the recipient of a Maria Moors Cabot Postdoctoral Research Fellowship at Harvard University. Additional financial support was provded in the form of operating research grants from the National Research Council of Canada to RLP, U.S. National Science Foundation, Research Grant BMS74-20563 to JGT, and the Maria Moors Cabot Foundation for Botanical Research of Harvard University. The authors also express their appreciation to Peter Del Tredici and Shirley LaPointe for growing the plants, Jean Brisson for helpful discussions about histochemistry, Gail Sugden for help and advice about SEM techniques, and Dr. B. Lu for use of his TEM.

AKKERMANS, A. D. L. 1971. Nitrogen fixation and nodulation of *Alnus* and *Hippophaë* under natural conditions. Ph.D. Thesis, Univ. Leiden, The Netherlands.

BECKING, J. H. 1975. Root nodules in non-legumes. *In* The development and function of roots. *Edited by* J. G. Torrey and D. T. Clarkson. Academic Press, London. pp. 507–566.

——— 1977. Endophyte and association establishment in non-

leguminous nitrogen-fixing plants. *In* Recent developments in nitrogen fixation. Proceedings of II International Symposium on Nitrogen Fixation, Salamanca, Spain. *Edited by* W. Newton, J. R. Postgate, and C. Rodriguez-Barrueco. Academic Press, London, England. pp. 551–567.

BECKING, J. H., W. E. DE BOER, and A. L. HOUWINK. 1964. Electron microscopy of the endophyte of *Alnus glutinosa*. Antonie van Leeuwenhoek; J. Microbiol. Serol. **30**: 343–376.

BOND, G. 1952. Some features of root growth in nodulated plants of *Myrica gale* L. Ann. Bot. **16**: 467–475.

——— 1974. Root-nodule symbioses with actinomycete-like organisms. *In* The biology of nitrogen fixation. *Edited by* A. Quispel. North-Holland Publishing Company, Amsterdam. pp. 342–378.

——— 1976*a*. The results of the IBP survey of root-nodule formation in non-leguminous angiosperms. *In* Symbiotic nitrogen fixation in plants. International Biological Programme 7. *Edited by* P. S. Nutman. Cambridge University Press, Cambridge, U.K. pp. 443–474.

——— 1976*b*. Observations on the root nodules of *Purshia tridentata*. Proc. R. Soc. London, Ser. B. **193**: 127–135.

——— 1977. Some reflections on *Alnus*-type root nodules. *In* Recent developments in nitrogen fixation. Proceedings of II International Symposium on Nitrogen Fixation, Salamanca, Spain. *Edited by* W. Newton, J. R. Postgate, and C. Rodriguez-Barrueco. Academic Press, London, England. pp. 531–537.

BOWES, B., D. CALLAHAM, and J. G. TORREY. 1977. Time-lapse photographic observations of morphogenesis in root nodules of *Comptonia peregrina* (Myricaceae). Am. J. Bot. **64**: 516–525.

BRISSON, J., R. L. PETERSON, J. ROBB, W. E. RAUSER, and B. E. ELLIS. 1977. Correlated phenolic histochemistry using light, transmission, and scanning electron microscopy, with examples taken from phytopathological problems. *In* Scanning electron microscopy—1977, Vol. II. Biological Applications of the SEM. *Edited by* O. Johari and R. P. Becker. Ill. Inst. Technol. Research Institute, Chicago, IL. pp. 667–676.

CALLAHAM, D., and J. G. TORREY. 1977. Prenodule formation and primary nodule development in roots of *Comptonia* (Myricaceae). Can. J. Bot. **55**: 2306–2318.

CHANDLER, M. R., and P. J. DART. 1971. *Casuarina* nodules. Report of the Rothamsted Experiment Station for 1971, part 1, p. 99.

CULLING, D. F. A. 1974. Modern microscopy: elementary theory and practice. Butterworths, London.

DALTON, D. A. and A. W. NAYLOR. 1975. Studies on nitrogen fixation by *Alnus crispa*. Am. J. Bot. **62**: 76–80.

DART, P. J. 1975. Legume root nodule initiation and development. *In* The development and function of roots. *Edited by* J. G. Torrey and D. T. Clarkson. Academic Press, London. pp. 467–506.

DEL TREDICI, P., and J. G. TORREY. 1976. On the germination of seeds of *Comptonia peregrina*, the sweet fern. Bot. Gaz. (Chicago), **137**: 262–268.

ERLANDSON, S. L., A. THOMAS, and G. WENDELSCHAFER. 1973. A simple technique for correlating SEM with TEM on biological material originally embedded in epoxy resin for TEM. *In* Scanning electron microscopy—1973, Vol. II. Biological applications of the SEM. *Edited by* O. Johari and I. Corvin. Ill. Inst. Technol. Research Institute, Chicago, IL. pp. 349–356.

FEDER, N., and T. P. O'BRIEN. 1968. Plant microtechnique: some principles and new methods. Am. J. Bot. **55**: 123–142.

FESSENDEN, R. J., R. KNOWLES, and R. BROUZES. 1973. Acetylene–ethylene assay studies on excised root nodules of *Myrica asplenifolia* L. Soil Sci. Soc. Am. Proc. **37**: 893–898.

FLETCHER, W. W., and I. C. GARDNER. 1974. The endophyte of *Myrica gale* nodules. Ann. Microbiol. **24**: 159.

FREUNDLICH, A., and A. W. ROBARDS. 1974. Cytochemistry of differentiating plant vascular cell walls with special reference to cellulose. Cytobiologie, **8**: 355–370.

GARDNER, I. C. 1965. Observations on the fine structure of the endophyte of the root nodules of *Alnus glutinosa* (L.) Gaertn. Arch. Mikrobiol. **51**: 365–383.

GARDNER, I. C., and E. M. S. GATNER. 1973. The formation of vesicles in the development cycle of the nodular endophyte of *Hippophaë rhamnoides* L. Arch. Mikrobiol. **89**: 233–240.

GARDNER, I. C. 1976. Ultrastructural studies of non-leguminous root nodules. *In* Symbiotic nitrogen fixation in plants. International Biological Programme 7. *Edited by* P. S. Nutman. Cambridge University Press, Cambridge, U.K. pp. 485–495.

GATNER, E. M. S., and I. C. GARDNER. 1970. Observations on the fine structure of the root nodule endophyte of *Hippophaë rhamnoides* L. Arch. Mikrobiol. **70**: 183–196.

HAWKER, L. E., and J. FRAYMOUTH. 1951. A re-investigation of the root-nodules of species of *Elaeagnus*, *Hippophaë*, *Alnus* and *Myrica*, with special reference to the morphology and life histories of the causative organisms. J. Gen. Microbiol. **5**: 369–386.

HOAGLAND, D. R., and D. I. ARNON. 1950. The water-culture method for growing plants without soil. Calif. Agric. Exp. Stn. Circ. 347 (Rev. ed.).

JUNIPER, B. E. 1976. Junctions between plant cells. *In* The developmental biology of plants and animals. *Edited by* C. F. Graham and P. F. Wareing. Blackwell Scientific Publications. Oxford, England. pp. 111–126.

KELLEY, R. O., R. A. F. DEKKER, and P. S. D. RHUNEN. 1973. Ligan-mediated osmium binding: its application in coating biological specimens for SEM. J. Ultrastruct. Res. **45**: 254–258.

LALONDE, M. 1977. Infection process of the *Alnus* root nodule symbiosis. *In* Recent developments in nitrogen fixation. Proceedings of II International Symposium on Nitrogen Fixation, Salamanca, Spain. *Edited by* W. Newton, J. R. Postgate, and C. Rodriguez-Barrueco. Academic Press, London, England. pp. 569–589.

LALONDE, M., and I. W. DEVOE. 1975. Scanning electron microscopy of the *Alnus crispa* var. *mollis* Fern. root nodule endophyte. Arch. Microbiol. **105**: 87–94.

——— 1976. Origin of the membrane envelope enclosing the *Alnus crispa* var. *mollis* Fern. root nodule endophyte as revealed by freeze-etching microscopy. Physiol. Plant Pathol. **8**: 123–129.

LALONDE, M. and R. KNOWLES. 1975*a*. Ultrastructure of the *Alnus crispa* var. *mollis* Fern. root nodule endophyte. Can. J. Microbiol. **21**: 1058–1080.

——— 1975*b*. Ultrastructure, composition, and biogenesis of the encapsulation material surrounding the endophyte in *Alnus crispa* var. *mollis* root nodules. Can. J. Bot. **53**: 1951–1971.

LALONDE, M., R. KNOWLES, and I. W. DEVOE. 1976. Absence of void area in freeze-etched vesicles of the *Alnus crispa* var. *mollis* Fern. root nodule endophyte. Arch. Microbiol. **107**: 263–267.

MITCHELL, J. P. 1965. The DNA content of nuclei in pea root nodules. Ann. Bot. N.S. **29**: 371–376.

NEWCOMB, W. 1976. A correlated light and electron microscopic study of symbiotic growth and differentiation in *Pisum sativum* root nodules. Can. J. Bot. **54**: 2163–2186.

NEWCOMB, W., K. SYŌNO, and J. G. TORREY. 1977. Development of an ineffective pea root nodule: morphogenesis fine structure and cytokinin biosynthesis. Can. J. Bot. **55**: 1891–1907.

SILVER, W. S. 1964. Root nodule symbiosis. I. Endophyte of *Myrica cerifera* L. J. Bacteriol. **87**: 416–421.

SKEFFINGTON, R. A., and W. D. P. STEWART. 1976. Evidence from inhibitor studies that the endophyte synthesises nitrogenase in the root nodules of *Alnus glutinosa* L. Gaertn. Planta (Berlin), **129**: 1–6.

STEWART, W. D. P., G. P. FITZGERALD, and R. H. BURRIS. 1967. *In situ* studies of $N_2$-fixation using the acetylene reduction technique. Proc. Natl. Acad. Sci., U.S.A. **58**: 2071–2078.

SYŌNO, K., W. NEWCOMB, and J. G. TORREY. 1976. Cytokinin production in relation to the development of pea root nodules. Can. J. Bot. **54**: 2155–2162.

TORREY, J. G. 1976. Initiation and development of root nodules of *Casuarina* (Casuarinaceae). Am. J. Bot. **63**: 335–344.

VAN DIJK, C., and E. MERKUS. 1976. A microscopical study of the development of a spore-like stage in the life cycle of the root-nodule endophyte of *Alnus glutinosa* (L.) Gaertn. New Phytol. **77**: 73–91.

VENABLE, J. H., and R. COGGLESHALL. 1965. A simplified lead citrate stain for use in electron microscopy. J. Cell Biol. **25**: 407–408.

ZIEGLER, H. 1960. "Rhizothamnien" bei *Comptonia peregrina* (L.) Coult. Naturwissenschaften, **5**: 113–114.

ZIEGLER, H., and R. HÜSER. 1963. Fixation of atmospheric nitrogen by root nodules of *Comptonia peregrina*. Nature (London), **199**: 508.

ZOBEL, R. W., P. DEL TREDICI, and J. G. TORREY. 1976. Method for growing plants aeroponically. Plant Physiol. **57**: 344–346.